PREPARATION, FUNCTIONALIZATION AND DERIVATIZATION OF NANOCRYSTALLINE CELLULOSE

A thesis submitted in partial fulfillment of the requirement for the degree of M. Phil. in Chemistry

SUBMITTED BY

MD. ABU HASAN HOWLADER

STUDENT ID: 0412033110

SESSION: APRIL 2012

Nano-Chemistry Research Laboratory
Department of Chemistry
Bangladesh University of Engineering and Technology
(BUET), Dhaka-1000, Bangladesh

May, 2015

Declaration by the Candidate

I do hereby declare that this thesis work, entitled "**Preparation, Functionalization and Derivatization of Nanocrystalline Cellulose**" submitted in partial fulfillment for the requirement of M. Phil. Degree in Chemistry to the Department of Chemistry, Bangladesh University of Engineering and Technology (BUET) in May 2015, is genuine work done by me under the supervision of Dr. Md. Shakhawat Hossain Firoz, Associate Professor of Chemistry, Bangladesh University of Engineering and Technology (BUET). The thesis or part of it has not been submitted before in any degree or diploma.

……

(Md. Abu Hasan Howlader)

Certificate

This is to certify that this thesis work entitled "**Preparation, Functionalization and Derivatization of Nanocrystalline Cellulose**" submitted by Md. Abu Hasan Howlader, Student ID: 0412033110, to the Department of Chemistry, Bangladesh University of Engineering and Technology (BUET) in partial fulfillment for the requirement of M. Phil. in Chemistry in May 2015 is based on his original research and investigation carried out under my guidance and supervision.

Supervisor:

……

Dr. Md. Shakhawat Hossain Firoz
Associate Professor
Department of Chemistry
Bangladesh University of Engineering and
Technology (BUET), Dhaka, Bangladesh

Bangladesh University of Engineering and Technology, Dhaka
Department of Chemistry

Certification of Thesis

A thesis on

PREPARATION, FUNCTIONALIZATION AND DERIVATIZATION OF NANOCRYSTALLINE CELLULOSE

BY

Md. Abu Hasan Howlader

has been accepted as satisfactory in partial fulfillment of the requirements for the degree of Master of Philosophy (M. Phil.) in Chemistry and certify that the student has demonstrated a satisfactory knowledge of the field covered by this thesis in an oral examination held on May 2, 2015

Board of Examiners

1. Dr. Md. Shakhawat Hossain Firoz
Associate Professor
Department of Chemistry
BUET, Dhaka
_____
Supervisor & Chairman

2. Dr. Md. Nazrul Islam
Professor & Head
Department of Chemistry
BUET, Dhaka Member
_____
(Ex-officio)

3. Dr. Shakila Rahman
Professor
Department of Chemistry
BUET, Dhaka
_____
Member

4. Dr. Md. Abdul Quader
Department of Chemistry
Professor
University of Dhaka, Dhaka
_____
Member (External)

DEDICATED TO

MY BELOVED PARENTS

&

RESPECTED MOTHER-IN-LAW

Acknowledgement

I would like to take this precious opportunity to thank my Supervisor, Dr. Md. Shakhawat Hossain Firoz for his guidance, knowledge and critical thinking have inspired me to dedicate myself to research work. I also would like thank Dr. Md. Nazrul Islam, Dr. Shakila Rahman, and Dr. Md. Abdul Quader, for their guidance, appreciated comments and help throughout this work.

I am indebted to many of my colleagues and respected teacher in department of chemistry, BUET. I would like to thank all my labmates and friends for their discussions and help. I would also like to thank all of the officers and staffs of the Department of Chemistry, BUET for their continuous help during my study period. I am grateful to the authority of BUET for providing financial support for this research work. I express my gratitude to department of Glass and Ceramic Engineering, BUET for giving support for FESEM analysis. I also thank Mr. Atique and to the authority of Bangladesh Atomic Energy Commission for helping XRD analysis. My deepest thanks go to my family and friends for their support throughout my life.

And finally, I would like to special thank my beloved wife, Merina pervin, for her support and patience during my research work and most importantly of all, for her unconditional love.

May 2015 Md. Abu Hasan Howlader

Abstract

Nanocrystalline cellulose (NCC) and its modified green products recently have gained the attention of the scientific community due to their potential applications in electronics, nanocomposite films, drug delivery, protein immobilization, metallic reaction template, pharmaceuticals, cosmetics, and personal cares. In this study, nanocrystalline cellulose (NCC) was prepared from microcrystalline cellulose (MCC) through strong acid hydrolysis viz. sulfuric acid, hydrochloric acid and a mixture of sulfuric acid and hydrochloric acid. It was observed that at H_2SO_4 concentration of 63% -65%, a clear stable transparent gel formed which on drying results transparent film. To functionalalize nanocrystalline cellulose, different chemical modifications like oxidation, reduction, schiff's base formation and hyrdazone formation were carried out.

NCC was converted to dialdehyde nanocellulose (DANC) with regioselective sodium meta periodate oxidizing agent. That dialdehyde nanocellulose was further converted to dicarboxylated and trihydroxyl nanocellulose with the selective sodium chlorite as oxidizing agent and sodium borohydride as reducing agent respectively. DANC was further derivatized with some primary aliphatic amines (ethylene diamine and hydroxyl amine hydrochloride) and some aromatic amines (aniline, 4-nitroaniline and 4-hydroxyaniline) via reductive amination.

Surface morphology and particle size were investigated through Field Emission Scanning Electron Microscopy (FESEM). The analysis showed that all the cellulosic materials are in the form of nanofiber and the average fiber diameter of NCC and other modified NCC were less than 20 nm with a length of 100 nm to few micrometers. The results of chemical analysis, FTIR and ^{1}HNMR spectra confirmed the conversion of NCC to different functional groups and amine derivatives. Thermogravimetric analysis results showed that the modified NCCs have higher thermal stability than NCC. The NCC and its all modified products are crystalline in nature where crystallinity index of modified NCCs was decreased compare to NCC. Surface charges were increased for the oxidized products of NCC. The optical transparency was examined in the visible range which showed that the transparency increased for all the modified NCC which suggests that all the modified NCCs are more dispersive than NCC in aqueous medium.

CONTENTS

LIST OF FIGURES

LIST OF TABLES

CHAPTER ONE

INTRODUCTION

1. Introduction

1.1 Introduction

Nanocrystalline cellulose (NCC) and its modified biodegradable products recently have received increasing interest in nanotechnology due to its advantages of abundance, renewability, and excellent mechanical properties and some potential applications in electronics, nanocomposite films, drug delivery, protein immobilization, metallic reaction template, pharmaceuticals, cosmetics, and personal cares [1-6]. Compared to cellulose fibres, NCC possesses many advantages; such as nanoscale dimension, high specific strength and modulus, high surface area, unique optical properties, etc [7-9]. These amazing physicochemical properties and wide application prospects have attracted significant interest from both research scientists and industrialists. Among the different methods for the preparation of NCC chemical method like acid hydrolysis is most promising [7, 10, 11]. Acid hydrolysis followed by ultrasonic treatment is also reported for the preparation of transparent aqueous gel of NCC [12]. It is well known that native cellulose consists with amorphous and crystalline regions.

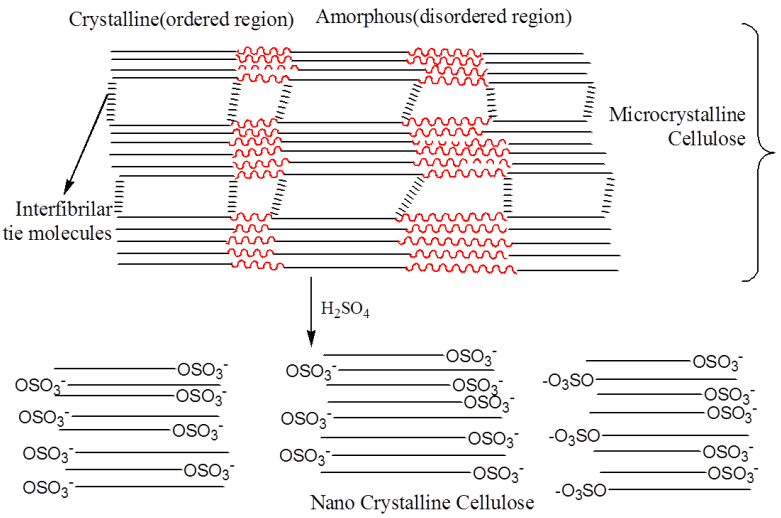

Fig. 1.1: Degradation of amorphous region of MCC by sulfuric acid

When native cellulose is subjected to harsh sulphuric acid treatment, the hydronium ions migrate to the amorphous regions since they have lower density compared to the crystalline regions. The hydronium ions cleave the glycosidic linkages hydrolytically thereby releasing the individual crystallites. Acid hydrolysis is dependent on different parameters, such as acid concentration, time of reaction, temperature of reaction and the specific acid used for the treatment [12]. Another important characteristic of NCC is that the individual crystallite has negative charges on their surface due to the formation of sulphate ester groups during sulfuric

acid treatment. The negatively charged NCC forms stable aqueous suspensions due to the electrostatic repulsion between the individual crystallites [13]. On the other hand, acid hydrolysis with hydrochloric acid does not produce as many negative surface charges on nanocrystalline cellulose, resulting in less stable NCC suspensions [14]. Nanocrystalline cellulose derived from acid hydrolysis of native cellulose possesses different morphologies depending on the origin and hydrolysis conditions. In order to characterize the morphology of NCC, various types of instruments can be used. The most conventional and common one is the transmission electron microscopy (TEM) [15], which can directly provide high-resolution images. Moreover, scanning electron microscopy (SEM) [16], atomic force microscopy (AFM) [17], small angle neutron scattering (SANS) [18] and polarized and depolarized dynamic light scattering (DLS, DDLS)[19] were also employed to study the morphology of NCC.

Despite many advantages of NCC, however, these fibers have certain limitations, which consequently hinder their potential applications. For example, they have limited thermal stability during composite processing [20, 21], limited matrix compatibility due to their highly hydrophilic character [22], and high moisture absorption of the fibers that can affect the dimensional and mechanical stability of the final products [21]. Attempts to rectify these shortcomings and make cellulose more conducive for different application means there is thus a great need to modify the cellulose and incorporate different functionality in it to make innovative materials. In the field of cellulose chemistry, numerous studies have been conducted within the last decades that have been aimed at searching for an appropriate application of cellulose for a variety of novel derivatives, or modification of the fibers themselves to provide them with specific properties like compatibility with composite material, hydrophobicity, and decrease in moisture absorption [23, 24].

As described earlier, to improve cellulose processability and to make new cellulose derivatives for specific industrial application, chemical modification of cellulose is a necessity. Cellulose can be derivatized in various ways by modifying its abundant hydroxyl groups. New functional groups can be introduced into cellulose through chemical modification; these functional groups can accordingly introduce new properties to the cellulose without destroying its many desirable intrinsic properties. This derivatization of cellulose would open windows of opportunities, broaden its use. Some of the original properties of cellulose can be altered by these chemical modifications. As cellulose is a carbohydrate polymer made up of repeating β-D-glucopyranose units and consists of three

hydroxyl groups per anhydroglucose unit (AGU) giving the cellulose molecule a high degree of functionality [25]. Oxidation is one of the important ways to incorporate new functionality in cellulose chain. However, most of the oxidation reaction is unselective. Depending on the nature of the oxidant and the reaction condition used, these oxidized celluloses may contain carboxylic, aldehyde, and/or ketone functionalities, in addition to the hydroxyl groups [26]. Though most of the chemical modifications of cellulose have been done on the primary hydroxyl groups at C-6 position like esterification, etherification, oxidation, etc., however, periodate can oxidize vicinal hydroxyl groups of cellulose at C-2 and C-3 positions to aldehyde groups, and at the same time cleave the corresponding carbon-carbon bond of the anhydro D-glucopyranose ring to form 2, 3-dialdehyde cellulose [27, 28].

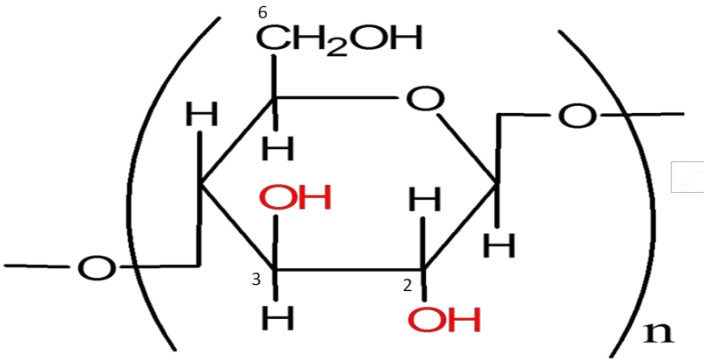

Fig. 1.2: Repeating glucose unit of nanocrystalline cellulose

The reaction proceeds under mild conditions and hence the amount of introduced aldehyde can be easily controlled [29]. Generally, amorphous regions are preferred by most chemical oxidations of cellulose in heterogeneous systems. In instances of periodate oxidation, however, crystalline domains are also affected and upon the introduction of aldehyde groups, crystallinity decreases with increasing level of oxidation [30]. Varma *et al*. reported that oxidized cellulose is thermally more stable than unmodified cellulose at higher temperature but less stable at lower temperatures below 25^0 C [31]. Moreover, upon the study of the morphology of the oxidized fibers it was found that the oxidized derivatives of cellulose showed a decreased aspect ratio when the cellulose samples were oxidized at a level of 30% [32].

The product of the selective oxidation, dialdehyde nanocellulose (DANC) can be further used as a chemical anchors for the incorporation of wide variety of functionalities in glucose unit of cellulose chain. For instance, dialdehyde can be further converted to carboxylic groups

[33], primary alcohols [34], or Schiff bases [35]. The reactivity of the dialdehyde functions allows for novel cellulose-based material with enhanced degradability and green characteristics. Consequently, this serves as a good vehicle for chemical derivatization.

Coupling of amine on to the modified fibers has been the topic of research for the past decade [29, 35, 36]. The Schiff base forming reaction between aldehyde and primary alkyl or aryl amine is a useful procedure to introduce these substituents. Dialdehyde cellulose can be coupled with amine derivatives and give rise to various nitrogen-containing derivatives in good yield by reaction at ambient temperature in a variety of solvents [35]. The nucelophilic addition reaction between a carbonyl group of dialdehyde cellulose and a primary amine results in a condensation product of imines [37]. Moreover, the same principle and mechanism is applied when a bifunctional amine such as ethylene diamine is used in the Schiff base reaction with dialdehyde cellulose. Schiff base derivative contain carbon-nitrogen double bond which can be easily oxidized in presence of oxygen or other oxidizing agent and this can overcome by *in-situ* reduction with a suitable reducing agent to stable secondary amine derivative. However, there haven't been many reports regarding the fabrication and characterization of these derivatives for specific applications. Recently, Kim *et al*. [29] studied the thermal decomposition of the resulting oxime and hydrazine derivatives of dialdehyde cellulose. These nitrogen-containing derivatives showed lower initial decomposition temperature and samples with higher degree of oxidations showed some explosive decomposition.

Consequently, the objectives of this research work are to

a. Prepare NCC from microcrystalline cellulose through acid hydrolysis process.

b. Functionalize NCC to dialdehyde nanocellulose, dicarboxylated acid and tri-hydroxyl nanocellulose.

c. Derivatize the dialdehyde nanocellulose into stable Schiff base derivatives with some aliphatic and aromatic primary amines.

d. Identify and characterize the functionalized and derivatized products.

1.2 References

1. Valo, H., Kovalainen, M., Laaksonen, P., Hakkinen, M., Auriola, S., Peltonen, L., Linder, M., Jarvinen, K., Hirvonen, J., & Laaksonen, T. 2011. *J Control Release*,. 156(3): 390-7.
2. Zimmermann, T., Bordeanu, N., & Strub, E. 2010. *Carbohydrate Polymers*, 79(4): 1086-1093.
3. Turbak, A. F., Snyder, F. W., & Sandberg, K.R. 1983. *Journal of Applied Polymer Science*, 37: 815-827.
4. Nogi, M., Iwamoto, S., Nakagaito, A. N., & Yano, H. 2009. *Advanced Materials*, 21(16): 1595-1598.
5. Syverud, K., & Stenius, P. 2009. *Cellulose*, 16(1): 75-85.
6. Favier, V., Chanzy, H., & Cavaille, J. Y. 1995. *Macromolecules*, *28*, 6365-6367.
7. De Souza Lima, M. M. & Borsali, R. 2004*Macromol. Rapid Commun,* 25, 771–787.
8. Lu P, & Hsieh, Y. L. 2010. Carbohyd Polym 82, 329-336.
9. Heux, L., Chauve, G., & Bonini C. 2000. *Langmuir*, 16:8210-8212.
10. Habibi, Y., Lucia, L. A., & Rojas, O. J. *Chem. Rev.* 2010, 110, 3479–3500.
11. Azizi Samir, M. A. S., Alloin, F., & Dufresne, A. 2005. *Biomacromolecules*, *6*, 612-626.
12. Bondeson, D., Mathew, A., & Oksman, K. 2006. *Cellulose, 13*, 171-180.
13. Lima, M. M. D., & Borsali, R. 2004. *Macromolecular Rapid Communications*, 25, 771-787.
14. Sugiyama, J., Vuong, R. & Chanzi, H. 1991. *Macromolecules,* 24, 4168-4175.
15. Araki, J., Wada, M., Kuga, S., & Okano, T. 1998. *Colloids Surf.* 142, 75–82.
16. Miller, A. F., & Donald, A. M., 2003. *Biomacromolecules,* 4, 510–517.
17. Pranger, L. & Tannenbaum, R. 2008. *Macromolecules* 41, 8682–8687.
18. Terech, P., Chazeau, L. & Cavaille, J. Y. 1999. *Macromolecules* 32, 1872–1875.
19. De Souza Lima, M. M. & Borsali, R. 2002. *Langmuir,* 18, 992–996.
20. Snijder, M. H. B., Wissing, E., & Modder, J. F. 1997. *Forest Products Society*, Madison, 5.
21. Woodhams, R. T., & Law, S. 1993. *Forest Product Society*, Madison.
22. Gatenholm, P., & Felix, J. 1993. *Forest Product Society*, Madison.
23. Belgacem, M. N., & Gandini, A. 2005. *Compos Interface.* 12(1–2), 41–75.
24. Li, S., Zhang, S., & Wang, X. 2008. *Langmuir*, 24, 5585–5590.
25. Klemm, D., Heublein, B., Fink, H. P., & Bohn, A. 2005. *Cellulose*, 44, 3358-93.

26. Nabar, G. M., & Padmanabhan, C. V. 1950. *Proceedings of the Indian Academy of Sciences: A*, 31, 371.
27. Jackson, E.J., & Hudson, C.S. 1937. *J. Am. Chem. Soc.*, 59, 2049.
28. Kim, U. J., Kuga, S., Wada, M., Okano, T., & Kondo, T. 2000. *Biomacromolecules,* , 1, 488.
29. Kim, U. J., & Kuga, S. 2001. *Thermochimica Acta*, 369, 79-85.
30. Varma, A.J., & Chavan, V.B. 1995. *Polymer Degradation and Stability*, 49, 245.
31. Varma, A.J., & Chavan, V.B. 1995. *Cellulose*, 2, 41.
32. Chavan, V.B., Sarwade, B.D., Varma, A.J. 2002. *Carbohydrate Polymers*, 50, 41.
33. Hofreiter, B. T.; Wolff, I. A. and Mehltretter, L. *J. Am. Chem. Soc*. 1957, 79, 6457.
34. Casu, B., Naggi, A., Torri, G., Allegra, G., Meille, S. V., Cosani, A., & Terbojevich, M. 1985. *Macromolecules,* 18, 2762.
35. Maekawa, E., & Koshijima, T. 1991. *J. Appl. Polym. Sci.* 42, 169.
36. Wu, M., & Kuga, S. 2006. *Journal of Applied Polymer Science*, 1668–1672.
37. Jerry, M. 1985. Advanced Organic Chemistry reactions, mechanisms and structure (3rd ed.). New York: John Wiley & Sons.

CHAPTER TWO

LITERATURE REVIEW

2. Literature Review

2.1 Structural properties and reactivity of cellulose

Cellulose is the most abundant natural biopolymer on earth, which is renewable, biodegradable, as well as non-toxic. Cellulose is a fibrous, tough, water-insoluble substance that plays an essential role in maintaining the structure of plant cell walls. It was first discovered and isolated by Anselme Payen in 1838 [1] and since then, multiple physical and chemical aspects of cellulose have been extensively studied; indeed, discoveries are constantly being made with respect to its biosynthesis, assembly, and structural features that have inspired a number of research efforts among a broad number of disciplines. Several reviews have already been published reporting the state of knowledge of this fascinating polymer [2-5]. Regardless of its source, cellulose can be characterized as a high molecular weight homopolymer of β-1,4-linked anhydro-D-glucose units in which every unit is corkscrewed180° with respect to its neighbors, and the repeat segment is frequently taken to be a dimer of glucose, known as cellobiose (Fig. 2. 1).

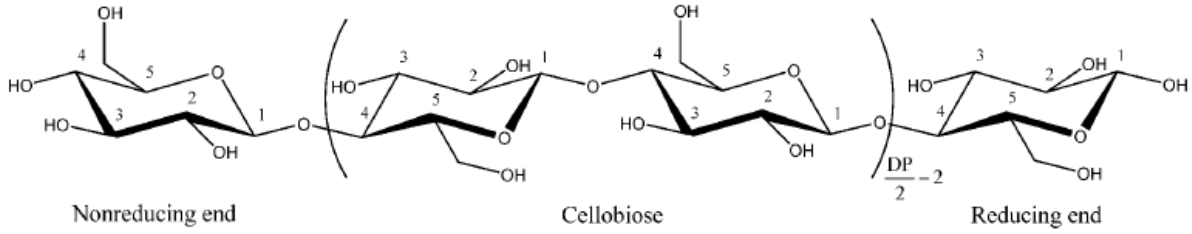

Fig. 2.1: Basic Chemical structure of cellulose showing the cellobiose repeat unit

Each cellulose chain possesses a directional chemical asymmetry with respect to the termini of its molecular axis: one end is a chemically reducing functionality (i.e., a hemiacetal unit) and the other has a pendant hydroxyl group, the nominal nonreducing end. The number of glucose units or the degree of polymerization (DP) is up to 20 000, but shorter cellulose chains can occur and are mainly localized in the primary cell walls. All -D-glucopyranose rings adopt a 4C1 chair conformation, and as a consequence, the hydroxyl groups are positioned in the ring (equatorial) plane, while the hydrogen atoms are in the vertical position (axial). This structure is stabilized by an intramolecular hydrogen bond network extending

from the O (3′)-H hydroxyl to the O (5) ring oxygen of the next unit across the glycosidic linkage and from the O(2)-H hydroxyl to the O(6′) hydroxyl of the next residue (Fig.2.2).

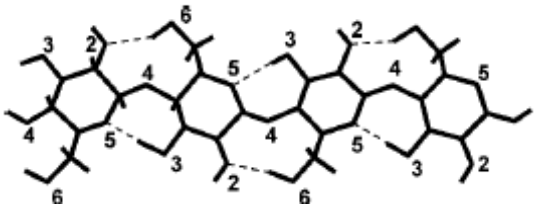

Fig. 2.2: Intramolecular hydrogen-bonding networks in a representative cellulose structure

In nature, cellulose does not occur as an isolated individual molecule, but it is found as assemblies of individual cellulose chain-forming fibers. This is because cellulose is synthesized as individual molecules, which undergo spinning in a hierarchical order at the site of biosynthesis. Typically, approximately 36 individual cellulose molecules assemble are brought together into larger units known as elementary fibrils (protofibrils), which pack into larger units called microfibrils, and these are in turn assembled into the familiar cellulose fibers. However, celluloses from different sources may occur in different packing as dictated by the biosynthesis conditions. The combined actions of biopolymerization, spinning, and crystallization occur in a rosette-shaped plasma membrane complex having a diameter of 30 nm (Fig.2.3) and are orchestrated by specific enzymatic *terminal complexes* (TCs) that act as biological spinnerets [6]. Because all the cellulose chains in one microfibril must be elongated by the complex at the same rate, crystallization during cellulose synthesis follows very closely polymerization of the chains by the TCs [7].

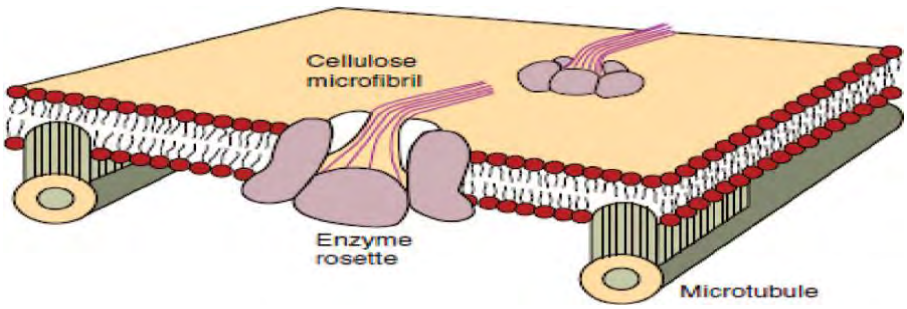

Fig. 2.3: Orientation of microtubules controlling the orientation of cellulose in the cell wall where the microtubules act like tracks to guide the cellulose enzymes floating in the cell membrane [8]

During the biosynthesis, cellulose chains are aggregated in microfibrils that display cross dimensions ranging from 2 to 20 nm, depending on the source of celluloses. The aggregation phenomenon occurs primarily via van der Waals forces and both intra- and inter-molecular hydrogen bonds (Fig. 2.2). If the TCs are not perturbed, they can generate a limitless supply of microfibrils having only a limited number of defects or amorphous domains [6, 9]. A number of models for the microfibril hierarchy have been proposed that attempt to describe the supramolecular structure of cellulose, including the crystalline structure, crystallite dimensions and defects, structural indices of amorphous domains, dimensions of fibrillar formation, etc. These models differ mainly in the description of the organization and the distribution of the amorphous or less ordered regions within the microfibril. After many years of controversy, it is common practice to acknowledge that the amorphous regions are distributed as chain dislocations on segments along the elementary fibril where the microfibrils are distorted by internal strain in the fiber and proceed to tilt and twist. [10] In the ordered regions, cellulose chains are tightly packed together in crystallites, which are stabilized by a strong and very complex intra- and intermolecular hydrogen-bond network. The hydrogen-bonding network and molecular orientation in cellulose can vary widely, which can give rise to cellulose polymorphs or allomorphs, depending on the respective source, method of extraction, or treatment [11]. Infra-red spectroscopy and x-ray diffraction studies of cellulose organization in plants have shown that the main portion of cellulose is constituted by crystallites with interspersed amorphous regions of low degree of order [12]. Native cellulose, namely cellulose I, is the crystalline cellulose. The term regenerated cellulose, also called cellulose II, is used to refer to cellulose precipitated out of solutions, generally alkali solutions [12]. These represent the two main polymorphs of cellulose. The current knowledge on the crystallography and biosynthesis of cellulose strongly suggests that the structure of cellulose is made up of parallel chains [13], whereas the crystalline structure of cellulose II is described as antiparallel [12]. Cellulose I is not the most stable form of cellulose. An additional hydrogen bond per glucose residue in cellulose II makes this allomorph the most thermodynamically stable form [14].

The chemical character and reactivity of cellulose is determined by the presence of three equatorially positioned OH groups in the AGU, one primary and two secondary groups [15]. In addition, the β-glycosidic linkages of cellulose are susceptible to hydrolytic attack [15].

The hydroxyl groups do not only play a role in the typical reactions of primary and secondary alcohols that are carried out on cellulose, but also play an important role in the solubility of cellulose. Cellulose is insoluble in common organic solvents and in water [15]. This is due to the fact that the hydroxyl groups are responsible for the extensive hydrogen bonding network forming both, intra- and intermolecular hydrogen bonding [16]. In order to dissolve cellulose, the prevailing hydrogen bonding network must be broken.

There are two possible mechanisms by which the OH groups in the cellulose molecule form hydrogen bonds. One is by the interaction between suitably positioned OH groups in the same molecule (intramolecular). These are located between C2-OH and C6-OH groups and C3-OH with endocyclic oxygen (Fig. 2.4. i and ii). The other mechanism occurs when neighbouring cellulose chains (intermolecular) interact via their C3-OH and C6-OH groups (Figure 1.4, iii). Intramolecular hydrogen bonds between the hydroxyl group at the C-3 and oxygen of the pyranose ring were first described in the 1960s by Liang and Marchessault, and Blackwell *et al.* who claimed the existence of a second 'pair' of intramolecular hydrogen bonds between the C-6 and C-2 of the neighboring AGUs [17].

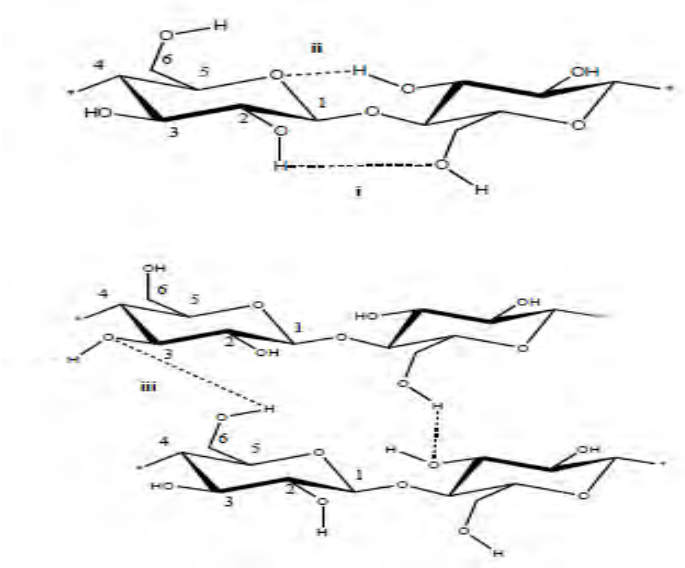

Fig. 2.4: Cellulose structures showing the intramolecular hydrogen bonding between (i) C2-OH and C6-OH (ii) C3-OH with endocyclic oxygen and (iii) the intermolecular hydrogen bonding between C3-OH and C6-OH

Cellulose is regarded as a semi-flexible polymer. The relative stiffness and rigidity of the cellulose molecule is mainly due to the intramolecular hydrogen bonding. This property is

reflected in its high viscosity in solution, a high tendency to crystallise, and its ability to form fibrillar strands. The chain stiffness property is further favoured by the β-glucosidic linkage that bestows the linear form of the chain. The chair conformation of the pyranose ring also contributes to chain stiffness. This is in contrast to the α-glucosidic bonds of starch.

2.2 Microcrystalline cellulose

Microcrystalline cellulose (such as Avicel) has a degree of polymerization (DP) value of less than 400 [18]. It can be prepared by treating different native cellulose sources such as wood pulp, bamboo, viscous rayon and cotton with mineral acids [19, 20]. The native cellulose has both amorphous and crystalline regions. The amorphous regions are interacted first with solvents and chemical reagents, because of their loose structures. The removal of the amorphous regions with an acid treatment of cellulose is the most commonly used method for the production of MCC. The acid hydrolysis breaks the β-(1→4) glycoside bond, thus decreasing the DP of the resulting MCC [21]. There are two types of MCC, powder MCC and colloidal MCC. Powder MCC is made by spray-drying of aqueous MCC suspension and has its average particle size ranging from about 20-90 μm. Colloidal MCC is MCC colloids in water with the colloidal size of <0.2μm in diameter [22]. MCC has excellent mechanical properties and can potentially be used as reinforcing fillers in polymer composites [23, 24]. MCC as a reinforcing filler in polymer composites offers several advantages over glass fibers and other inorganic fillers: renewability, nonfood sources, low energy required for its production, low cost, low density, and high specific strength and modulus [25]. Like other inorganic fillers such as glass fibers, MCC fillers have hydrophilic surfaces and are not very compatible with hydrophobic plastics. Coupling agents or compatibilizers are often required for improving the bonding between MCC and the plastic matrix [26]. Moreover, the processing temperature of MCC-filled composites is restricted to about 200 °C because MCC starts to degrade near 230 °C, whereas glass-fiber-reinforced composites can have a much higher processing temperature [27].

2.3 Nanocrystalline Cellulose

Nanocrystalline cellulose (NCC) refers to rigid rod-like crystals produced by sulphuric acid treatment of native cellulose. There are basically two families of nanosized cellulosic particles. The first one consists of cellulose nanocrystals and the second one is microfibrillated cellulose (MFC). However, cellulose nanocrystals are often referred to as microcrystals, whiskers, nanocrystals, nanoparticles, microcrystallites, or nanofibers [28]. In the 1950s, Ranby reported for the first time that colloidal suspensions of cellulose can be obtained by controlled sulfuric acid-catalyzed degradation of cellulose fibers [29]. This work was inspired by the studies of Nickerson and Habrle [30] who observed that the degradation induced by boiling cellulose fibers in acidic solution reached a limit after a certain time of treatment. A recent review from Habibi *et al.* [31] gives a clear overview of such cellulosic nanomaterials. Simultaneously, the development by Battista [32] of the hydrochloric acid-assisted degradation of cellulose fibers derived from high-quality wood pulps, followed by sonification treatment, led to the commercialization of microcrystalline cellulose (MCC).

As native cellulose consists of amorphous and crystalline regions [14, 33] when native cellulose is subjected to harsh sulphuric acid treatment, the hydronium ions migrate to the amorphous regions since they have lower density compared to the crystalline regions. The hydronium ions cleave the glycosidic linkages hydrolytically thereby releasing the individual crystallites (Fig. 2.5). Acid hydrolysis is dependent on different parameters, such as acid concentration, time of reaction, temperature of reaction and the specific acid used for the treatment. Dong *et al.* [34] were among the first researchers to study the effect of hydrolysis conditions on the properties of resulting cellulose nanocrystals. They proved that longer hydrolysis time leads to shorter monocrystals and also to an increase in their surface charge. Beck-Candanedo *et al.* [35] also studied the properties of cellulose nanocrystals obtained by hydrolysis of softwood and hardwood pulps. They studied the influence of hydrolysis time and acid-to-pulp ratio in order to obtain cellulose nanocrystals. They explained that the reaction time is one of the most important parameters to be considered in the acid hydrolysis of wood pulp. Moreover, they reported that too long reaction times completely digest the cellulose to yield its component sugar molecules. Nanocrystalline cellulose derived from acid hydrolysis of native cellulose possesses different morphologies depending on the origin and hydrolysis conditions. NCCs are rigid rod-like crystals with diameter in the range of 10–20nm and lengths of a few hundred nanometers were obtained by using a 63.5 % (w/w) sulfuric acid concentration for approximately 2 h (Fig. 2.6 and 2.7) and which can be

prepared from a variety of sources, e.g., microcrystalline cellulose [34], bacterial cellulose [36], algal cellulose (valonia) [37], hemp [38], tunicin [39], cotton [40], ramie [41], sisal [42], sugar beet [43], and wood [35].

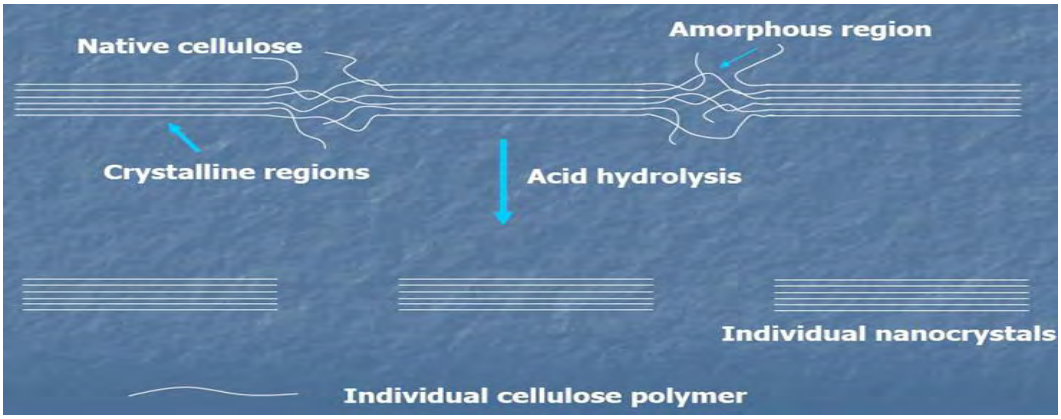

Fig. 2.5: Sulphuric acid treatment of native cellulose

Dufresne [44] reported that the stability of nanocrystal suspensions depends on the dimensions of their dispersed particles, their size polydispersivity and their surface charge. Araki *et al.* [45] compared the effects of using sulfuric acid or hydrochloric acid to produce stable suspensions of cellulosic nanocrystals. They explained that sulfuric acid provides more stable aqueous suspensions than hydrochloric acid. According to the same authors, hydrochloric acid produced cellulose nanocrystals with minimum surface charge. On the contrary, sulfuric acid-prepared nanocrystals present a negatively charged surface [35], due to the esterification of surface hydroxyl groups to give charged sulfate groups during acid treatment, which enhances their stability in aqueous solutions. [35]. In order to characterise the morphology of NCC, various types of instruments can be used. The most conventional and common one is the transmission electron microscopy (TEM) which can directly provide high-resolution images. Moreover, scanning electron microscopy (SEM) , atomic force microscopy (AFM) , small angle neutron scattering (SANS) and polarised and depolarized dynamic light scattering (DLS, DDLS) were also employed to study the morphology of NCC.

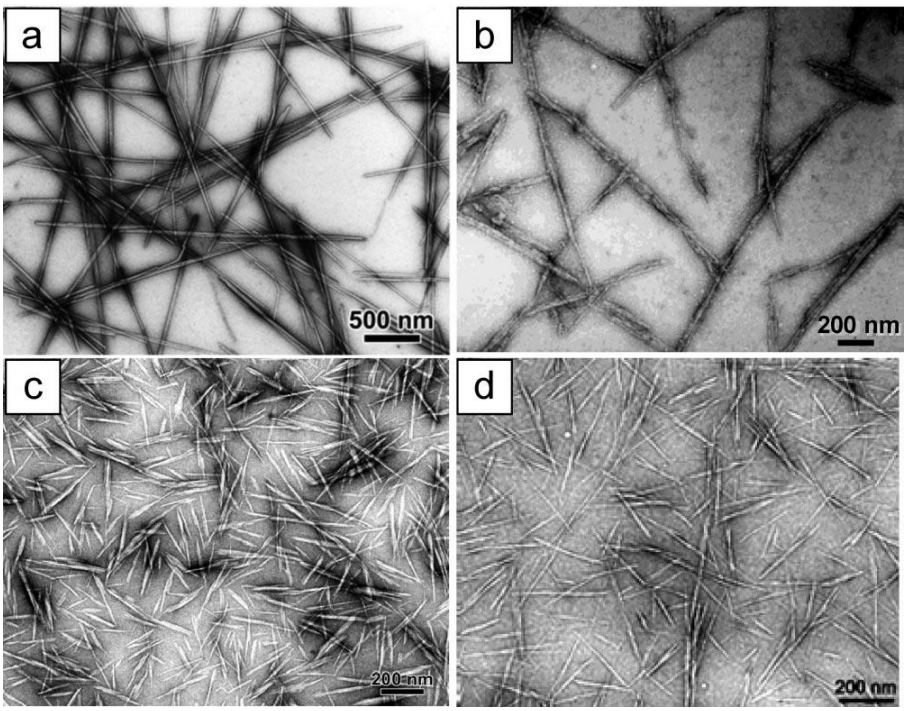

Fig. 2.6: TEM images of dried dispersion of cellulose nanocrystals derived from (a) tunicate [46], (b) bacterial [47], (c) ramie [41], and (d) sisal [42].

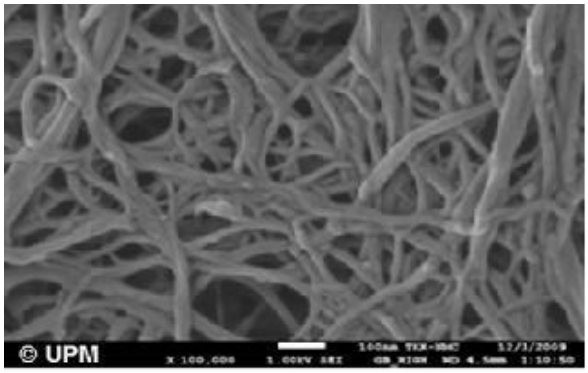

Fig.2.7: FESEM image of Nanofibrilation cellulose [48].

2.4 Preparation of Cellulose Nanocrystals

The main process for the isolation of CNs from cellulose fibers is based on acid hydrolysis. Disordered or paracrystalline regions of cellulose are preferentially hydrolyzed, whereas crystalline regions that have a higher resistance to acid attack remain intact [49]. Thus, following an acid treatment that hydrolyzes the cellulose (leading to removal of the microfibrils at the defects), cellulose rod-like nanocrystals are produced. The actual occurrence of the acid cleavage event is attributed to differences in the kinetics of hydrolysis between amorphous and crystalline domains [50]. This hypothesis was based on the reasonable assumption that disordered or para-crystalline domains are regularly distributed along the microfibers and therefore they are more susceptible to acid attack (in contrast to crystalline regions that are more impervious to attack). Also, homogeneous crystallites were supposed to be generated after acid hydrolysis. These assumptions were actually confirmed by X-ray crystal diffraction [51], electron microscopy with iodine-staining [52], small-angle X-ray diffraction [53], and neutron diffraction analyses [51]. Typical procedures currently employed for the production of CNs consist of subjecting pure cellulosic material to strong acid hydrolysis under strictly controlled conditions of temperature agitation, and time. The nature of the acid and the acid-to-cellulosic fibers ratio are also important parameters that affect the preparation of CNs. A resulting suspension is subsequently diluted with water and washed with successive centrifugations. Dialysis against distilled water is then performed to remove any free acid molecules from the dispersion. Additional steps such as filtration [46], differential centrifugation [54], or ultracentrifugation [55] have been also reported.

Sulfuric and hydrochloric acids have been extensively used for CN preparation, but phosphoric [56] and hydrobromic [57] acids have also been reported for such purposes. If the CNs are prepared by hydrolysis in hydrochloric acid, their ability to disperse is limited and their aqueous suspensions tend to flocculate [45]. On the other hand, when sulfuric acid is used as a hydrolyzing agent, it reacts with the surface hydroxyl groups of cellulose to yield charged surface sulfate esters that promote dispersion of the CNs in water [58]. However, the introduction of charged sulfate groups compromises the thermostability of the nanocrystals [47]. Post-treatment of CNs generated by hydrochloric acid hydrolysis with sulfuric acid has been studied to introduce, in a controlled fashion, sulfate moieties on their surfaces [59]. CNs generated from hydrochloric acid hydrolysis and then treated with sulfuric acid solution had the same particle size as those directly obtained from sulfuric acid hydrolysis; however, the

surface charge density could be tuned to given values by sulfuric acid hydrolysis. With respect to the morphology of the particles, a combination of both sulfuric and hydrochloric acids during hydrolysis steps appears to generate spherical CNs instead of rod-like nanocrystals when carried out under ultrasonic treatment [60]. These spherical CNs demonstrated better thermal stability mainly because they possess fewer sulfate groups on their surfaces [61].

The concentration of sulfuric acid in hydrolysis reactions to obtain CNs does not vary much from a typical value of 65% (w/w); however, the temperature can range from room temperature up to 70 °C and the corresponding hydrolysis time can be varied from 30 min to overnight depending on the temperature. In the case of hydrochloric acid-catalyzed hydrolysis, the reaction is usually carried out at reflux temperature and an acid concentration between 2.5 and 4 N with variable time of reaction depending on the source of the cellulosic material. Bondenson et al. [62] investigated optimizing the hydrolysis conditions by an experimental factorial design matrix (response surface methodology) using MCC that was derived from Norway spruce (*Picea abies*) as the cellulosic starting material. The factors that were varied during the process were the concentrations of MCC and sulfuric acid, the hydrolysis time and temperature, and the ultrasonic treatment time. The responses that were measured were the median size of the cellulose particles and the yield of the reaction. The authors demonstrated that with a sulfuric acid concentration of 63.5% (w/w) over a time of approximately 2 h, it was possible to obtain CNs having a length between 200 and 400 nm and a width less than 10 nm with a yield of 30% (based on initial weight). Prolongation of the hydrolysis time induced a decrease in nanocrystal length and an increase in surface charge [34]. Reaction time and acid-to-pulp ratio on nanocrystals obtained by sulfuric acid hydrolysis of bleached softwood (black spruce, *Picea mariana*) sulfite pulp was investigated by Beck-Candanedo et al. [35]. They reported that shorter nanoparticles with narrow size polydispersity were produced at longer hydrolysis times. Recently, Elazzouzi-Hafraoui et al. [46] studied the size distribution of CNs resulting from sulfuric acid hydrolysis of cotton treated with 65% sulfuric acid over 30 min at different temperatures, ranging from 45 to 72 °C. By increasing the temperature, they demonstrated that shorter crystals were obtained; however, no clear influence on the width of the crystal was revealed.

2.5 NCC in dry state

NCC is normally processed and stored as an aqueous suspension. This is done to avoid the agglomeration of the fibers during drying, caused by a phenomenon called hornification. The hornification defines irreversible changes in the natural structure of the fibers upon water removal [63]. It can be explained by an increased degree in crosslinking in the material microstructure due to the formation of a large number of hydrogen bonds between the hydroxyl groups of neighboring fibers [64]. Since this process is irreversible once dried, the material cannot be resuspended in water. This property has been used for the production of different dried forms of NCC. Hence, NCC has been converted into dry state to form aerogels, films and powders. When the water is removed from NCC gel by freeze-drying, highly porous (250-389 m2/g), flexible and deformable aerogels are formed [65]. These kinds of gels have been studied for numerous applications (e.g. drug delivery, catalysis, filtrations, grafts, cushioning and liquid storage) [66]. Diluted NCC suspensions have been converted to a dried powder form by spray drying [67]. The most studied dry forms of NCC are NCC films produced by filtration method [68], molding [69, 70] or spin coating [71]. When water is removed by any of these methods, films with tight fiber networks of high strength are formed. These films are sometimes referred to as nanofiber paper or nanopaper [68, 69, 71]. Depending on the diameter of the NCC fibers the films show different degree of transparency which can be as high as 90 % [72, 73]. Their application is based on their high strength and good barrier properties [68]. However, the high hydrophilicity of NCC limits wide utilization of films made of pure NCC in some areas (e.g. in packaging). Thus, composite type films are often prepared by mixing NCC with other polymers [74].

2.6 Selective functionalization of cellulose

Periodate oxidation can cleave C2–C3 bonds of β-D-glucose monomer units of cellulose [75] and selectively oxidize C-2 and C-3 vicinal hydroxyl groups to form 2, 3-dialdehyde units along the cellulose chains [76]. The 2, 3-dialdehyde groups can be further oxidized to form 2, 3- dicarboxyl groups by sodium chlorite in an aqueous acid medium [77, 78]. However, these oxidation treatments cause many changes in the structure and crystallinity of cellulose. Varma et al., Varma and Chavan and Saito et al. found that for oxidized celluloses the crystallinity decreased with increasing oxidation level of the original cellulose [79, 80]. Chavan et al. investigated the morphology of oxidized cellulose [81]. From scanning electron microscopy (SEM) images, they found that all the cellulose fibers of oxidized derivatives showed a decreased aspect ratio when the cellulose samples were oxidized at a level of 30 % (based on glucose units). Kim et al. also reported that the crystallinity of cellulose oxidized by periodate oxidation was decreased with increasing oxidation level, and furthermore, they found that the dialdehyde groups were highly unevenly distributed on longitudinally spaced and bandlike domains of cellulose fibers [82].

2.7 Schiff base derivatization of dialdehyde cellulose

Many different cellulose derivatives have been produced by a variety of chemical modifications. Periodate oxidized dialdehyde cellulose can be potentially useful for further modifications to carboxylic acids [78], primary alcohols [83], or imines [84] from its intrinsic reactivity with primary amines. Grafting and coupling of amine on to the modified fibers has been the topic of research for t he past decade [84, 85]. The Schiff base forming reaction between aldehyde and primary alkyl amine is a useful procedure to introduce these substituents. Cellulose can be coupled with amine derivatives and give rise to various nitrogen containing derivatives in good yield by reaction at ambient temperature in different solvents [84]. The nucelophilic addition reaction between a carbonyl group of dialdehyde cellulose and a primary amine followed by transfer of a proton from nitrogen to oxygen results in a stable Schiff base. When a carbonyl group is introduced adjacent to the nitrogen atom, the electrophilic reactivity of an imine (or iminium ion) is greatly enhanced [86].

2.8 Applications of cellulose, nanocellulose and cellulose derivatives

Cellulose is a versatile starting material for several applications. It is directly linked to the paper industry in which cellulose is used in a conventional way, as a structural material for paper and cardboard products. However, even though this is the current major use of cellulose, only the imagination is the limit for the utilization of this extremely versatile and adaptable material. Cellulose can be chemically modified to yield derivatives which are used widely in different industrial sectors in addition to conventional applications. As an example, in 2003, 3.2 million tons of cellulose was used as a raw material in the production of regenerated fibres and films in addition to cellulose derivatives. Derivatives are further used as coatings, laminations, optical films and absorbents. Additionally, cellulose derivatives can be found as additives in building materials and also in pharmaceutical, food and cosmetic products [87]. MCC is used in the pharmaceutical industry as a tablet excipient due to its beneficial properties such as zero toxicity, hygroscopicity, chemical inactivity and reversible adsorbency. It is also used as tablet binder and diluent in wet granulation or in direct compression, and as a tablet disintegrant, anti-adherent or capsule diluents [88].

Pure nanocellulose is harmless for people and it is biocompatible. Therefore it can be used for health care application, personal hygiene products, cosmetics and biomedicine. One of the simplest applications of NCC dispersions is its use for stabilization of medical suspensions against phase separation and sedimentation of heavy ingredients. Chemically modified nanocellulose can be a promising carrier for immobilization of enzymes and other drugs. Due to its nano size, such a carrier-drug complex can penetrate through skin pores and treat skin diseases. Moreover, it can be used a gentle, but active peeling agent in cosmetics. Cellulose-based Nanomaterials a sustainable and renewable material (however living sources from which they are extracted are sustainable and renewable, not the natural fibres or nanoparticles [90] have been of increasing interest as potential nano-reinforcing filler into biocomposites for industrial and biomedical applications. They have low density, high aspect ratio, good mechanical properties, low thermal expansion, low toxicity, surfaces having hydroxyl groups (-OH) that can be readily chemically functionalized [74, 90, 91, 92]. These nanomaterials have been extensively studied for a wide variety of potential applications such as nanofillers for polymer nanocomposites, protective coatings, barrier/separation membranes and filtration

systems, scaffolds for tissue engineering, transparent films, antimicrobial films, pharmaceuticals, drug delivery, organic solar cells, supercapacitors, substrates for flexible electronics, and lithium-ion batteries etc. [87, 92].

2. 9 References

1. Payen, A. 1838. *Compt. Rend.*, *7*, 1052.
2. Hon, D. N. S., & Shiraishi, N. 1991. *Wood and Cellulosic Chemistry*; Marcel Dekker, Inc.: New York.
3. Marchessault, R. H., & Sundararajan, P. R. 1983. .In *The Polysaccharides*; Aspinall, G. O., Ed.; Academic Press: New York.
4. O'Sullivan, A. C. 1997. *Cellulose*, *4*, 173.
5. Salmon, S., & Hudson, S. M. 1997. *Polym. Re*V., *37*, 199.
6. Brown, R. M. J. *J.* 1996. *Macromol. Sci., Part A: Pure Appl. Chem.*, *A33*, 1345.
7. Williamson, R. E., Burn, J. E., & Hocart, C. H. 2002. *Trends Plant Sci.*, *7*, 461.
8. Vincent, J. F. V. 2002. *Mater. Today*, *5*, 28.
9. Brown, R. M. J. *J.* 2004, *Polym. Sci., Part A: Polym. Chem.*, *42*, 487.
10. Rowland, S. P., & Roberts, E. J. 1972. *J. Polym. Sci., Part A: Polym. Chem.*, *10*, 2447.
11. Atalla, R. H. 1984. *Struct., Funct., Biosynth. Plant Cell Walls, Proc. Annu. Symp. Bot., 7th*, 381.
12. Daniel, J. R. 1985. Cellulose structure and properties. In *Encyclopedia of Polymer Science and Engineering*; Kroschwitz, J.I., Ed.; Wiley-Interscience Publication John Wiley & Sons: New York, NY, USA, 3, 86-123.
13. Dinand, E., Vignon, M., Chanzy, H., & Heux, L. 2002. *Cellulose,* 9, 7-18.
14. Saxena, I. M., Brown, R. M. 2005. J. *Ann. Bot.*, *96*, 9-21.
15. Klemm, D., Philipp, B., Heinze, T., Heinze, U., & Wagenknecht, W. 1998. *Comprehensive Cellulose Chemistry*, *Volume 1, Fundamentals and Analytical Methods*, Wiley-VCH, Weinheim.
16. Krässig, H. 1996. *Cellulose, Polymer Monographs Volume 11*, Gordon and Breach Science Publishers, Amsterdam, 6-42.
17. Machessault, R., & Liang, C. 1960. *J. Polym. Sci.*, 43, 71.
18. Klemm, D., Heublein, B., Fink, H. P., & Bohn, A. 2005. *Cellulose*, 44, 3358-3393.
19. Battista, O.A., & Smith, P.A., 1962. *J. Ind. Eng. Chem.*, 54, 20-29.
20. Sun, Y., Lin, L., Deng, H., Li, J., He, B., Sun, R., & Ouyang, P. 2008. *BioResources*, 3, 297-315.

21. Hakansson, H., & Ahlgren, P.2005. Cellulose, 12, 177- 183.
22. Gan, L.X., Whistler, R.L., *Carbohydr Res,* 1990, 206, 65-69.
23. Helbert, J. Y.C.A.D. 1996. *Polymer Composites*, 17, 604 611.
24. Qiu, W., Zhang, F., Endo, T., & Hirotsu, T., 2003. *Journal of Applied Polymer Science*, 87, 337-345.
25. Azizi Samir, M.A.S., Alloin, F., & Dufresne, A. 2005. *Biomacromolecules*, 6, 612-626.
26. Amash, A., Hildebrandt, F. I., & Zugenmaier, P. 2002. *Designed Monomers & Polymers* 5, 385-399.
27. Ardizzone, S., Dioguardi, F.S., Mussini, T., Mussini, P.R., Rondinini, S., Vercelli, B., & Vertova, A., 1999. *Cellulose*, 6, 57-69.
28. Dufresne, A. 2008. Cellulose-based composites and nanocomposites. In *Monomers, Polymers and Composites from Renewable Resources*, 1st ed.; Gandini, A., Belgacem, M.N., Eds.; Elsevier: Oxford, UK, 401-418.
29. Rånby, B. G. 1949. *Acta Chem. Scand.*, *3*, 649.
30. Nickerson, R. F., & Habrle, J. A. 1947. *Ind. Eng. Chem.*, *39*, 1507.
31. Habibi, Y., Lucia, L. A., & Rojas, O. J. 2010. Chem. Rev. 110, 3479–3500.
32. Battista, O. A. *Ind. Eng. Chem.* 1950, *42*, 502.
33. Sugiyama, J., Vuong, R., & Chanzi, H. 1991. *Macromolecules*, *24*, 4168-4175.
34. Dong, X. M., Revol, J.F., & Gray, D. 1998. *Cellulose*, *5*, 19-32.
35. Beck-Candanedo, S., Roman, M., & Gray, D. 2005. *Biomacromolecules*, *6*, 1048-1054.
36. Hirai, A., Inui, O., Horii, F., & Tsuji, M. 2009. *Langmuir*, *25*, 497-502.
37. Sugiyama, J., Chanzi, H., & Revol, J.F. 1994. *Planta,* 193, 260-265.
38. Cao, X., Chen, Y., Chang, P. R., Stumborg, M., & Huneault, M. A. 2008. *J. Appl. Polym. Sci.*, *109*, 3804-3810.
39. Bonini, C., Heux, L., Cavaille, J.Y., Lindner, P., Dewhurst, C., & Terech, P. 2002, *Langmuir*, *18*, 3311-3314.
40. Thielemans, W., Warbey, C. R., & Walsh, D. A. 2009. *Green Chem*, *11*, 531-537.
41. Habibi, Y., Goffin, A. L., Schiltz, N., Duquesne, E., Dubois, P., & Dufresne, A. 2008. *J. Mater. Chem.*, *18*, 5002-5010.
42. Garcia de Rodriguez, N. L., Thielemans, W., Dufresne, A. 2006, *Cellulose*, *13*, 261-270.

43. Azizi Samir, M.A.S., Alloin, F., Paillet, M., Dufresne, A. 2004. *Macromolecules*, *37*, 4313-4316.
44. Dufresne, A. Polymer nanocomposites from Biological Sources. In *Encyclopedia of Nanoscience and Nanotechnology*, 2nd ed.; Nalwa, H.S., Ed.; American Scientific Publisher: Valencia, CA, USA; in press.
45. Araki, J., Wada, M., Kuga, S., Okano, T.1998. Colloids Surf. Physicochem. Eng. Aspects 142, 75–82.
46. Elazzouzi-Hafraoui, S., Nishiyama, Y., Putaux, J. L. Heux, L., Dubreuil, F., & Rochas, C. 2008. *Biomacromolecules, 9*, 57.
47. Roman, M., & Winter, W. T. 2004. *Biomacromolecules*, *5*, 1671.
48. Vartiainen, J., Pöhler, T., Sirola, K., Pylkkänen, L., Alenius, H., Hokkinen, J., Tapper, U., Lahtinen, P., Kapanen, A., Putkisto, K., Hiekkataipale, P., Eronen, P., Ruokolainen, J., & Laukkanen, A. 2011. Cellulose, 18(3), 775-786.
49. Angles, M. N., & Dufresne, A. 2001, *Macromolecules*, *34*, 2921.
50. Håkansson, H., Ahlgren, P. 2005. *Cellulose*, *12*, 177.
51. Nishiyama, Y., Kim, U. J., Kim, D. Y., Katsumata, K. S., May, R. P., & Langan, P. 2003. *Biomacromolecules*, *4*, 1013.
52. Schurz, J., John, K. 1975.Cellul. *Chem. Technol.*, *9*, 493.
53. Yachi, T. Hayashi, J., Takai, M., & Shimizu, Y. 1983. *J. Appl. Polym. Sci.: Appl. Polym. Symp.*, *37*, 325.
54. Bai, W., Holbery, J., & Li, K. 2009. *Cellulose*, *16*, 455.
55. De Souza Lima, M. M., Wong, J. T., Paillet, M., Borsali, R. & Pecora, R. 2003. Langmuir, 19, 24–29.
56. Koshizawa, T. 1960. *Kami Pa Gikyoshi*, *14*, 455.
57. Filpponen, I. 2009. Ph.D. Thesis, North Carolina State University, Raleigh, NC.
58. Revol, J. F., Bradford, H., Giasson, J., Marchessault, R. H., & Gray, D. G. 1992. *Int. J. Biol. Macromol*, *14*, 170.
59. Araki, J., Wada, M., Kuga, S., Okano, T. 2000. *Langmuir*, *16*, 2413.
60. Wang, N., & Ding, E., Cheng, R. 2008. *Langmuir*, *24*, 5.
61. Wang, N., & Ding, E., Cheng, R. 2007. *Polymer*, *48*, 3486.
62. Bondeson, D., & Mathew, A. Oksman, K. 2006. *Cellulose*, *13*, 171.
63. Fernandes Diniz, J. M. B., Gil, M. H., & Castro, J. A. A. M. 2004. *Wood Science and Technology*, 37(6), 489-494.
64. Hult, E. L., Larsson, P. T., & Iversen, T. 2001. *Polymer*, 42(8), 3309-3314.

65. Paakko, M., Ankerfors, M., Kosonen, H., Nykanen, A., Ahola, S., Osterberg, M., Ruokolainen, J., Laine, J., Larsson, P. T., Ikkala, O., & Lindstrom, T. 2007. *Biomacromolecules*, 8(6), 1934-1941.
66. Liu, S., Yan, Q., Tao, D., Yu, T., & Liu, X. 2012. *Carbohydrate Polymers*, 89(2), 551-557.
67. Peng, Y., Gardner, D. & Han, Y. 2012. *Cellulose*, 19(1), 91-102.
68. Nogi, M., Iwamoto, S., Nakagaito, A.N., & Yano, H. 2009. *Advanced Materials*, 21(16), 1595-1598.
69. Syverud, K., & Stenius, P. 2009. *Cellulose*, 16(1), 75-85.
70. Andresen, M., Stenstad, P., Moretro, T., Langsrud, S., Syverud, K., Johansson, L. S., & Stenius, P. 2007. *Biomacromolecules*, 8(7), 2149-55.
71. Aulin, C., Ahola, S., Josefsson, P., Nishino, T., Hirose, Y., Osterberg, M., & Wagberg, L. 2009. *Langmuir*, 25(13), 7675-85.
72. Nogi, M., & Yano, H. 2009. *Applied Physics Letters*, 94(23).
73. Fukuzumi, H., Saito, T., Iwata, T., Kumamoto, Y., & Isogai, A., 2008, *Biomacromolecules*, 10(1), 162-165.
74. Siro, I., & Plackett, D. 2010. *Cellulose*, 17(3), 459-494.
75. Bruneel, D., & Schacht, E. 1993. *Polymer*, 34, 2628–2632.
76. Hou, Q. X., Liu, W., Liu, Z. H., & Bai, L. L. 2007. *Ind Eng Chem Res*, 46, 7830–7837.
77. Maekawa, E., & Koshijima, T. 1984. *J Appl Polym Sci*, 29(7), 2289–2297.
78. Hofreiter, B. T., Wolff, I. A., & Mehltretter, L. 1957. *J Am Chem Soc,* 79, 6457–6460.
79. Varma, A. J., Chavan, V. B., 1995. *Polym Degrad Stab,* 49, 245 250.
80. Varma, A. J., Chavan, V. B. 1995. *Cellulose,* 2, 41–49.
81. Chavan, V. B., Sarwade, B. D., & Varma, A. J. 2002. *Carbohydr Polym* ,50, 41–45.
82. Kim, U. J., Kuga, S., Wada, M., Okano, T., & Kondo, T. 2000. *Biomacromolecules* 1, 488–492.
83. Casu, B., Naggi, A., Torri, G., Allegra, G., Meille, S. V., Cosani, A., & Terbojevich, M. 1985. *Macromolecules*, 18, 2762.
84. Maekawa, E., Koshijima, T., J. 1991. *Appl. Polym. Sci.,* 42, 169.
85. Kim, U. J., & Kuga, S. 2001. *Thermochimica Acta*, 369, 79-85.
86. Jacobi, A., Wangelin, V., Neumann, H., Gordes, D., Klaus, S., Strubing, D., & Beller, M. 2003. Chem. Eur. J., 9, 4286-4294.

87. Podsiadlo, P., Choi, S., Shim, B., Lee, J., Cuddihy, M., & Kotov, N. A. 2005. *Biomacromolecules,* 6, 2914-2918.
88. Shangraw, R.F., & Dermarest, D. 1993. *Pharm Tech*, 17(1), *32*-44.
89. Faruka, O., Bledzki, A. K., Fink, H. P., & Sain, M. 2012. *Prog. Polym. Sci.,* 37, 1552-1596.
90. Lin, N., Huang, J., & Dufresne, A. 2012. *Nanoscale,* 4, 3274-3294.
91. Moon, R.J., Martini, A., Nairn, J., Simonsen, J., & Youngblood, J. 2011. *Chem. Soc. Rev.,* 40, 3941-3994.
92. Hu, L., Zheng, G., Yao, J., Liu, N., Weil, B., Eskilsson, M., Karabulut, E., Ruan, Z., Fan, S., Jason, T., Bloking, J. T., McGehee, M.D., Wågberg, L., & Cui. Y. 2013. *Energy Environ. Sci.,* 6, 513-518.

CHAPTER THREE

EXPERIMENTAL

3. Experimental

3.1 Materials

MCC (Merck, Germany) was used as starting cellulose material. 98% (w/w) H_2SO_4 was also purchased from Merck, Germany and all other chemicals were purchased from Sigma-Aldrich or Fisher and used as received unless otherwise stated. Deionized water was used throughout the experiments.

3. 2 Preparation of NCC through H_2SO_4 hydrolysis

Although there are several preparation techniques of NCC is known, even that it was optimized by the variation of acid concentration, MCC to acid ratio, hydrolysis time, temperature of hydrolysis and ultrasonic time and power. Based on the physical appearance of the prepared NCC gel and its film transparency optimum hydrolysis conditions were selected for the preparation of NCC. The procedure was as follows: A 500 mL round bottom flask containing 10 g of microcrystalline cellulose (MCC) was placed in an oil bath at a 60 ^{o}C temperature. Simultaneously, 200 mL 63.5 % (w/w) H_2S0_4 (MCC-to-acid weight ratio of 1 to 20) was adjusted to the temperature desired. When the two substances reached working temperature, H_2SO_4 was mixed with the cellulose, and the mixture was hydrolyzed at 60 ºC temperature for 90 minutes with continuous stirring with a magnetic stirrer. The ultrasonication was applied during (every 30 minutes) the reaction while cooling in an ice bath to avoid overheating. Immediately following hydrolysis, the suspension was diluted ten-fold to stop the reaction and allowed to settle for several hours until the suspensions were layered, and the clear top layer was decanted off, and then repeatedly washed with distilled water until they were not layered. The suspension was then transferred into centrifuge tubes and repeated centrifugation was performed at 4,000 rpm for 10 minutes to remove excess acid and water-soluble fragments. The fine cellulose particles became dispersed in the aqueous solution approximately at pH 4. The turbid supernatant containing the polydisperse cellulose particles was then collected for further centrifugation at 4000 rpm for 45 minutes to separate the NCC suspension. The suspension was then washed with deionized water. The process was repeated four to five times for each sample to reduce the acid content. Afterward, the resulting suspension was placed in regenerated cellulose dialysis tubes having a molecular weight cutoff of 12,000– 14,000 and dialyzed against deionized (DI) water for several days

until the water pH remained constant. The purified NCC suspension was kept in a refrigerator at 5 ^{o}C. Some fraction of dialyzed NCC was dried in freeze dryer for the preparation of powdered sample.

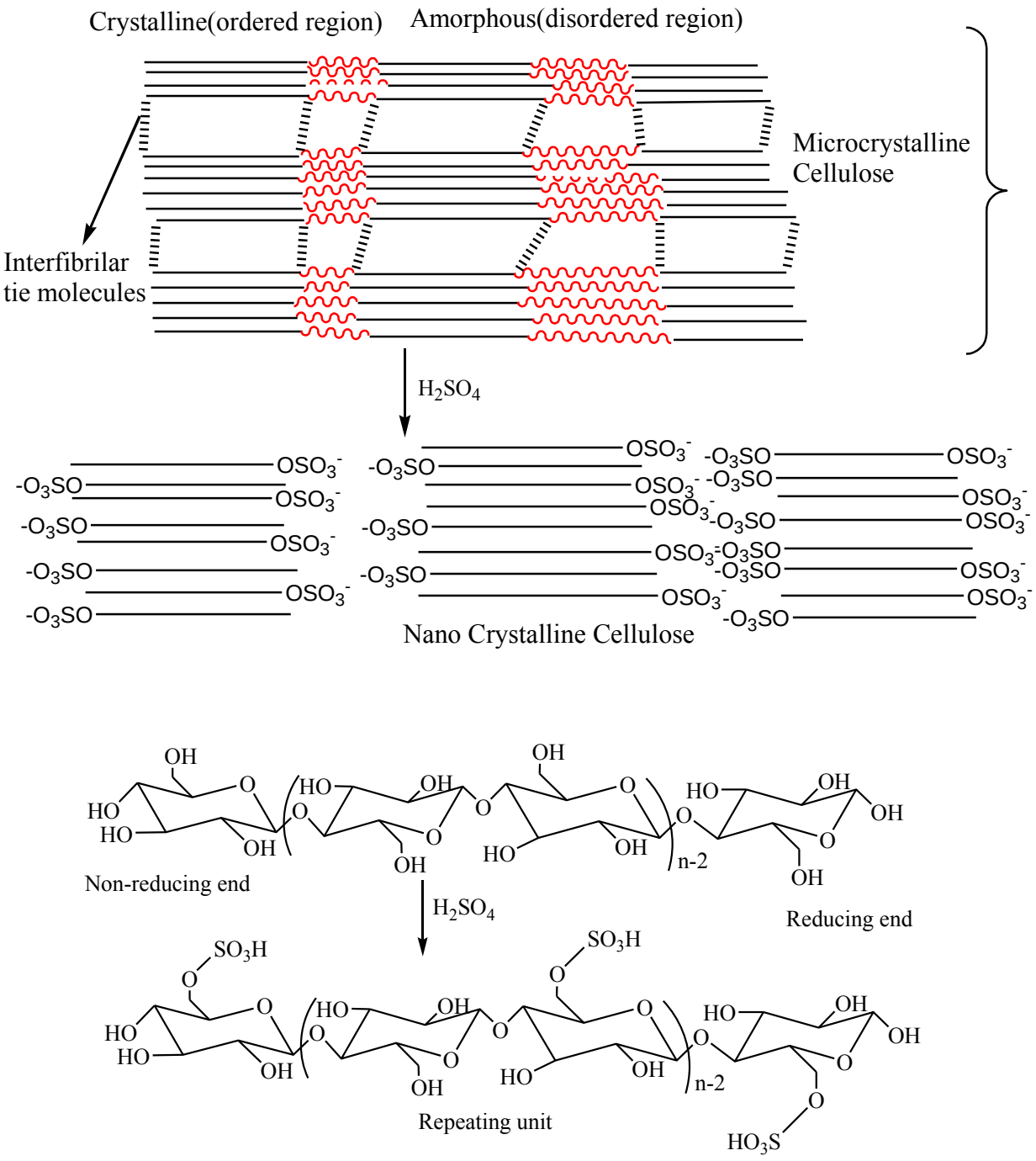

Fig 3.1: Hydrolysis of Microcrystalline Cellulose with H_2SO_4

3.3 Preparation of NCC through HCl hydrolysis

The hydrochloric acid hydrolysis was carried out with 6N HCl at 80 ^{o}C for three hours and other condition and processes were same as H_2SO_4 hydrolysis.

3.4 Preparation of NCC through mixture of HCl and H_2SO_4 hydrolysis

10 g MCC were transferred into an acidic aqueous solution consisting of 200 mL mixed acid made of 120 mL DI water, 20 mL 37% (w/w) HCl and 60 mL 98% (w/w) H_2SO_4 (6: 1: 3) and this suspension was hydrolyzed for 8 hours at 60 ^{o}C temperature with periodic sonication (every 30 minitues) in a ultrasonicator with an internal heater at 80 ^{o}C, during which the mixture was stirred vigorously with a mechanical stirrer. After the hydrolysis process, the mixture turned into milky colloid suspension. The mixture was then transferred into centrifuge bottles and centrifuged. The products were continuously washed by addition of DI water and repeated centrifugation. The fine cellulose particles become dispersed in the aqueous solution approximately at pH 4. Afterward, the fractions were dialyzed (Sigma-Aldrich, dialysis membrane MWCO: 12000-14000) against DI water. The thoroughly washed products were freeze dried and stored at 5^{0}C for further testing.

3.5 Preparation of CNC films

The suspensions of NCCs after being stored in a refrigerator at 5 ^{o}C for 2 days were poured into polystyrene Petri dishes, which were then kept in the vacuum evaporator at 40 ^{o}C for slow water evaporation. Solid thin films were obtained after evaporation. All films were kept in desiccators for further characterization.

3.6 Functionalization of NCC

3.6.1 Selective oxidation with Sodium meta periodate

An aqueous mixture of nanocellulose (500 mL, 2 %, w/v) and sodium periodate (13.38 g) was stirred for 20 hours in the absence of light at 48 ^{o}C temperature controlled oil bath with a magnetic stirrer. After the reaction was stopped with excess ethylene glycol, the sample was washed with distilled water by repeated centrifugation. The product was then placed into dialysis membranes (MWCO: 12000–14,000) and dialyzed against DI water for several days to remove the unwanted ions. 20 mL aqueous suspension dialdehyde product was dried at 40 ^{o}C in vacuum oven to constant weight for subsequent analysis. The oven dired product was formed a thin transparent film. Some fractions of the product were freeze dried and it gave powdered sample. Other fractions were stored for identification of carbonyl group and for determination of aldehyde content.

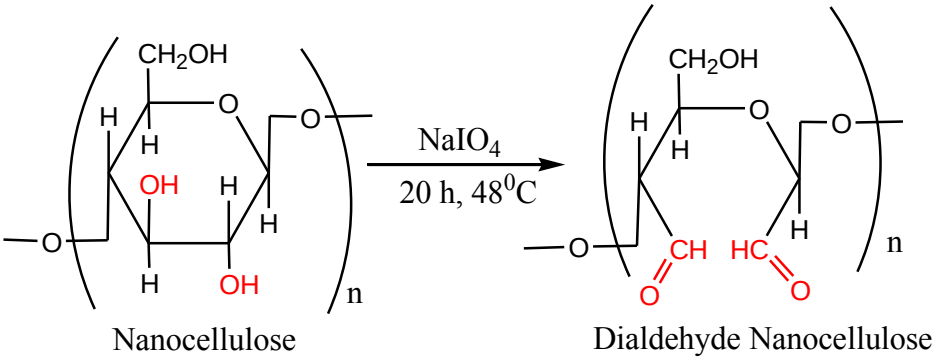

Nanocellulose Dialdehyde Nanocellulose

Fig.3.2: conversion of nanocrystalline cellulose to dicarboxylated nanocellulose

3.6.2 Determination of carbonyl groups

3.6.2.1 Copper titration

The carbonyl group content of the starting and oxidized NCC was determined following Tappi standard method T430 (Tappi Standard T430). Briefly, DANC (0.182 g) were treated with an aqueous $CuSO_4$ solution (5.0 mL, 0.40 N) and a carbonate-bicarbonate solution (90 mL, 2.40 N, 1.04 N). The mixture was heated to 100 ^oC for 3 h, cooled, filtered, and washed with 5 % aqueous Na_2CO_3 solution (100 mL, w/v) and hot DI water (150 mL). The product along with the filter paper were dispersed in 5 % phosphomolybdic acid (24 mL, w/v), stirred, filtered, and then washed thoroughly with water. The filtrate was diluted with deionized water (450 mL) followed by the titration with 0.0488 N $KMnO_4$ to a faint pink end point. A blank test was also performed following the same procedure. Each set of the test was done in triplicate.

The copper number was calculated using equation

$$\text{Copper number (Cu} \neq) = \frac{6.36 \times (\text{V} - \text{B}) \times \text{N} \times 100}{\text{W}} - - - - - - 3.1$$

Where:

V = the volume of $KMnO_4$ solution to titrate the filtrate from the specimen, mL.

B = the volume of $KMnO_4$ solution to titrate the blank filtrate, mL.

N = Normality of $KMnO_4$, 0.0488 N.

W = the weight of pulp fibers, g.

The copper number is an indication of aldehyde groups in fibers. It has been

Reported that there is a linear relationship between the carbonyl group content and copper number

Carbonyl Group Content (mmol /100 g sample) = (Cu# − 0.07) / 0.6

3.6.2.2 Oxime formation method

Dialdehyde groups can be converted to oximes by a Shiff base reaction with hydroxylamine hydrochloride. The aldehyde content of oxidized cellulose was determined by the hydroxylamine hydrochloride method. 0.182 g of dialdehyde nanocellulose suspension was taken 100 mL beaker and the pH was adjusted to 3.5 with HCl. The pH of the hydroxylamine

hydrochloride solution (5 %, w/w) was also adjusted to 3.5 before it was added to the suspension. The pH of this suspension was always kept at 3.5 by adding 0.1314 M NaOH until no decrease of pH was observed. Here, the volume consumption of NaOH solution in liter was recorded as Vc. The same concentration of NCC suspension at pH 3.5 was used as a blank and its volume consumption of the alkali solution in liter was recorded as V_b. Thus the aldehyde content (AC) in DANC can be calculated by

$$AC\ (\%) = \frac{M_{NaOH} \times (V_c - V_b) \times}{m/160} \quad \text{---------} \quad 3.2$$

Where M_{NaOH} = 0.1314 M, m is the dry weight of DANC sample in g, and 160 is approximately the molecular weight of repeating unit in DANC. Each set of the test was done in triplicate.

3.7 Chlorite oxidation process for preparation of dicarboxylated nanocellulose

150 mL (1.2225 g) of periodate oxidized NCC suspension was taken in a round bottom flask, and 4.0 g NaCl, 2.0 g $NaClO_2$ and 5.0 mL H_2O_2 were added into this mixture. The mixture was stirred for 24 h at a speed of 400 rpm at room with a magnetic stirrer. This regioselective oxidation routes introduce anionic groups into the cellulose structure. After 24 h, the reaction mixture turned into yellow color solution without any solid product. Then ethanol was slowly added to the clear reaction mixture, some transparent gelatinous precipitate formed which were separated by centrifugation. Again ethanol was slowly added to the supernatant until no further precipitation was observed.

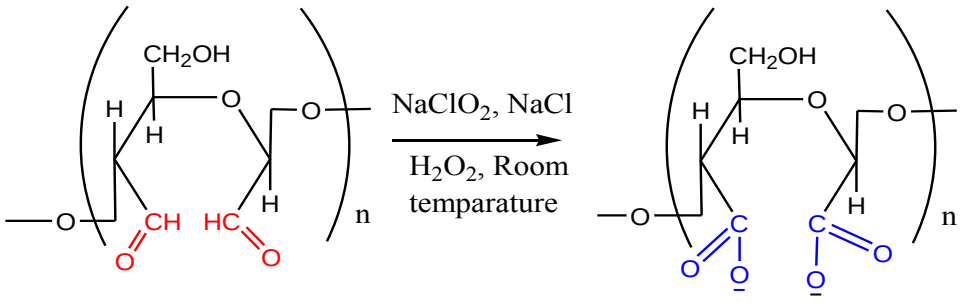

Fig. 3.3: Conversion of dialdehyde nanocellulose to dicarboxylated nanocellulose

3.8 Preparation of Tri-hydroxyl nanocellulose

50 mL (0.455 g) DANC suspension was taken in a round bottom flask and 50 mL (0.20 g) $NaBH_4$ was added into suspension. The mixture was stirred for 24 h at a speed of 400 rpm at room with a magnetic stirrer. After the reaction the product was collected by repeated washing and centrifugation.

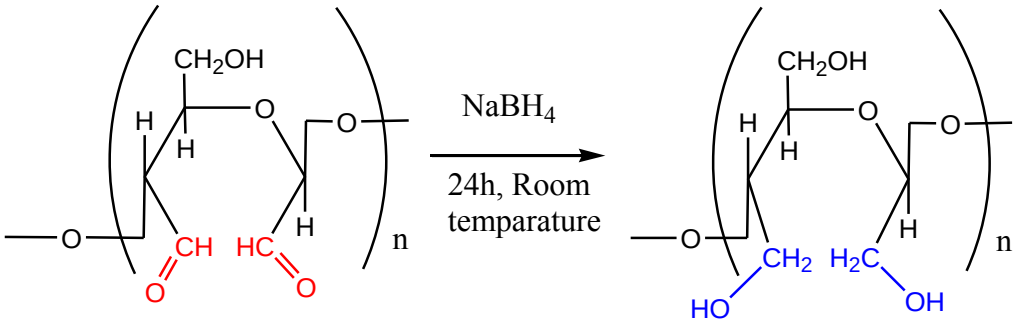

Dialdehyde Nanocellulose

Tri-hydroxyl Nanocellulose

Fig. 3.4: Conversion of dialdehyde nanocellulose to trihydroxyl nanocellulose

3.9 Derivatization of NCC

3.9.1 Reaction of dialdehyde nanocellulose with amines

20 mL (0.182 g) dialdehyde nanocellulose suspension was taken in a round bottom flask and stirred for 15 min at 70^0C. 2.0 mL Ethylene diamine, 1.0 g hydroxyl amine hydrochloride, 2.0 mL aniline, 1.0 g nitro aniline and 1.0 g 4-hydroxy aniline were then slowly added to the suspension in separate experiments and the mixture was continuously stirred at70 ^{o}C for 3 h followed by the *in situ* reduction of the resulting imine intermediate at room temperature employing 0.5 g $NaBH_4$ dissolved in 25 mL DI water. After stirring for 3h, the product was washed with distilled water by repeated centrifugation with mixture of ethanol DI water and dialyzed (MWCO: 12000–14,000) against and DI water until the pH was neutral and subsequently, the slurry was freeze dried to obtain the dry product with a yield of 80–90 %. On the other hand some portion of the slurry was dried in vacuum oven at 40 ^{o}C to prepare thin film. The freeze dried and oven dried products were stored in desiccator for further analysis and testing.

A schematic pathway for oxidation and reductive amination of dialdehyde nanocellulose is shown in the following Scheme.

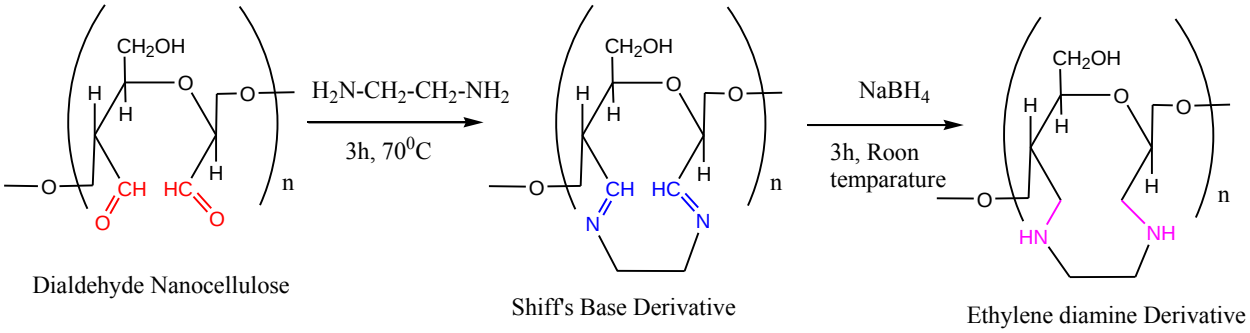

Fig. 3.5: Reductive amination of dialdehyde nanocellulose with ethylenediamine

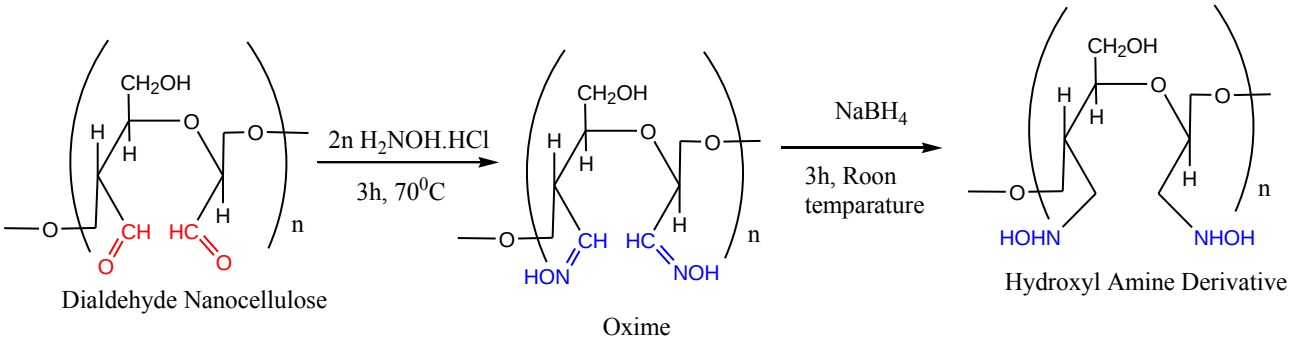

Fig. 3.6: Reductive amination of dialdehyde nanocellulose with hydroxylamine

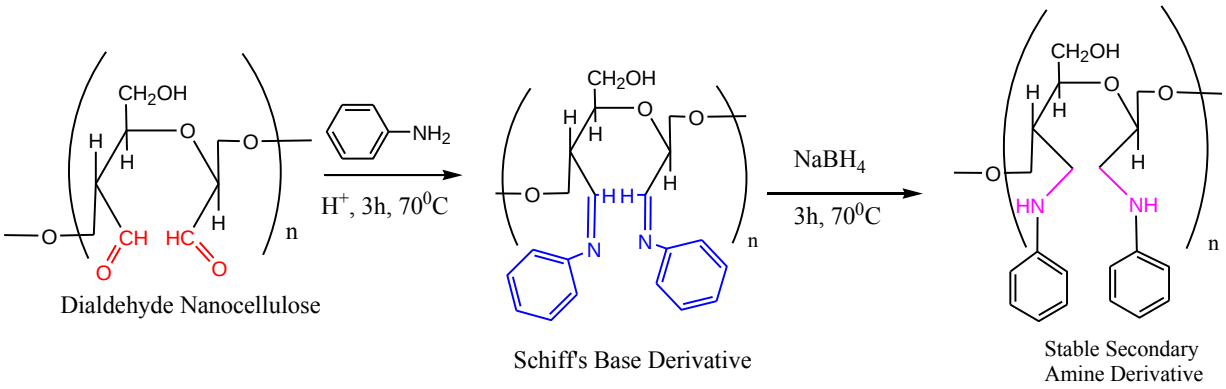

Fig. 3.7: Reductive amination of dialdehyde nanocellulose with aniline

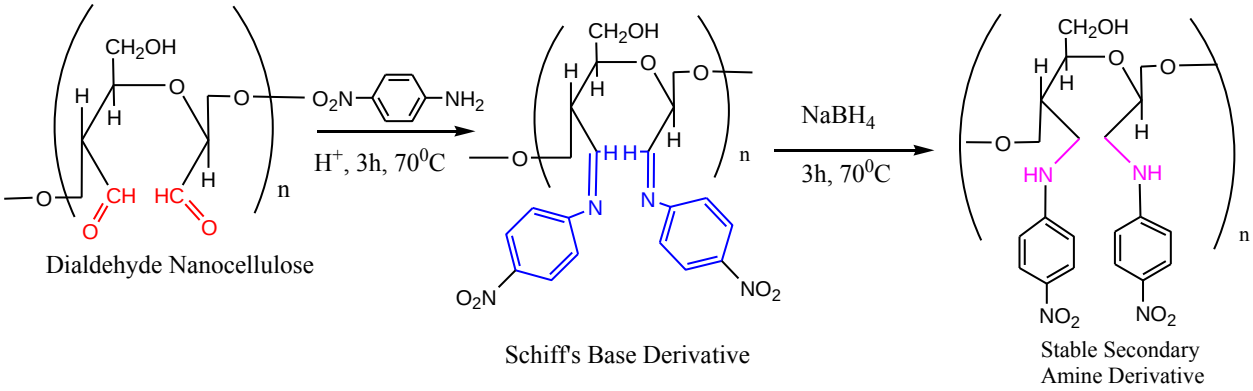

Fig. 3.8: Reductive amination of dialdehyde nanocellulose with 4-nitroaniline

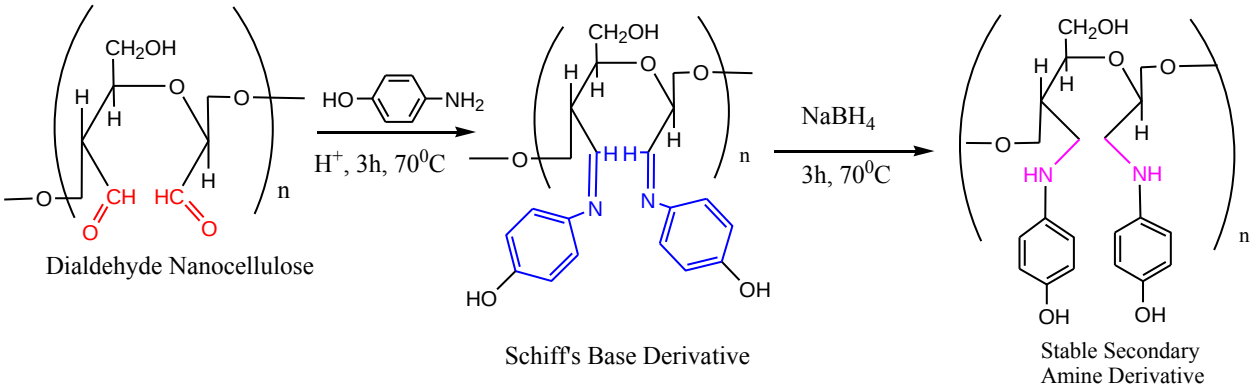

Fig. 3.8 Reductive amination of dialdehyde nanocellulose with 4-hydroxyaniline

2.10 Characterization

3.10.1 Determination of point of zero charge (pH_{pzc})

The surface charge (Q) and the pHpzc of the prepared NCC and functionalized NCC in aqueous phase were analyzed with different system pH value by using the titration method. 50 mg dried NCC and functionalized NCC were taken in 50 mL 0.1 M NaCl solution separately and suspended by ultrasonic sound for 30 minutes. Then 10.0 mL 0.01M HCl added into the mixture which was agitated with a magnetic stirrer for 3h. The titration was carried out with 0.01 M NaOH solution and the pH of the solution measured after an equilibrium time of 5 minutes.

3.10.2 X-ray diffraction (XRD)

It is well known that the mechanical properties of cellulose products were strongly dependent on the crystallinity and crystal structure. To determine the crystal structure and crystallinity, XRD patterns of the MCC, NCC, and chemically modified NCCs were measured by automated powder X-ray diffractometer. Before testing, all freeze dried powder samples were dried in a vacuum oven at 50 ˚C for 24 h to remove moisture. The powder samples were pressed in a square aluminum sample holder (40mm X 40mm) with a 1 mm deep rectangular hole (20mm x 15mm) and pressed against an optical smooth glass plate. The upper surface of the sample was labeled in the plane with its sample holder. The sample holder was then placed in the diffractometer. The WXRD data were generated by a diffractometer with Cu-Ka radiation (λ = 1.542˚ A) at 40 kV and 30 mA over the range $2\theta = 10^{\circ}–50^{\circ}$, a size step of 0.02˚, and a time step of 2.0 s, (1.0 h per scan.

The degree of crystallization was determined using the method of X-ray Crystallinity index. The formula below was used in calculating degree of crystallization.

$$\text{Crystallinity index} = \frac{I_{002} - I_{am}}{I_{002}} \quad \text{----------3.3}$$

Where I_{002} represents the diffraction intensity of crystallization at the 002 peak and I_{am} represents the diffraction intensity of amorphous region.

3.10.3 Scanning electron microscopy

Morphological analysis was performed using Field Emission Scanning Electron Microscopy (FESEM). A drop of dilute suspension was deposited on small piece of carbon strip and allowed to dry at vacuum drier at 40 ^{o}C. The sample surface was coated with a thin layer of gold to provide electrical conductivity. The sample was then placed in the main SEM chamber to view its surface. The system was computer interfaced and thus provides recording of the surface images in the computer file for its use as hard copy.

3.10.4 Fourier transform infrared measurement

The starting MCC and all other prepared NCC or modified NCC samples were dried in a vacuum oven at 50 ^{o}C for 24 hours and then cooled to room temperature for Fourier transform infrared (FTIR) analysis. The oven dried film of NCC and its modified films were analyzed by single bounce diamond ATR (Attenuated Total Reflectance) accessory and the freeze dried samples were pressed into KBr pellets (1:200). Transmission mode of FTIR spectra were collected with Shimadzu IR spectrometer. Spectra were obtained in 400-4000 cm^{-1} range and for each sample 45 scans were taken at a resolution of 4 cm^{-1}.

3.10.5 Proton Nuclear Magnetic Resonance (^{1}H-NMR) spectroscopy

Liquid ^{1}H-NMR spectra of freeze dried NCC and modified NCCs were obtained on a Bruker 400 MHz system, operating at a frequency 400.17 MHz at room temperature. Freeze dried samples were suspended in deuterium oxide by high ultrasonic sound for 30 minutes around 30 ^{o}C temperature by adding ice. An aliquot of this suspension (0.5mL) was transferred to an NMR tube and 128 scans were collected for each spectrum.

3.10.6 Ultraviolet – visible spectra

The ultraviolet-visible spectra of the NCC and modified NCCs film were taken by a double beam spectrophotometer in transmission mode for the determination of transparency of the films. The sample film was placed in the sample holder while the reference holder was vacant. The spectrophotometer was attached with a synchronized personal computer (PC) for recording the spectral data. All the analysis was performed at room temperature.

3.10.7 Thermogravimetric analysis

The thermal stability of MCC, NCC and modified NCCs were studied by a thermo-gravimetric analyzer (TGA) in a nitrogen atmosphere. Approximately 5 mg oven dried film samples in a platinum pan were heated from 30 to 600 ^{o}C at a heating rate of 10°C/min under a nitrogen flow of 60mL min^{-1}. Before the data acquisition segment, the sample was equilibrated at 25 ^{o}C for 5 min to obtain an isothermal condition. The weight-loss rate was obtained from derivative thermo-gravimetric (DTG) data.

CHAPTER FOUR

RESULTS AND DISCUSSION

4. Results and Discussion

4.1 Acid hydrolysis of microcrystalline cellulose

A number of different factors affecting the acidic hydrolysis of cellulose were examined. A complete set of investigated parameters include: reaction time and temperature, acid concentration, ratio of MCC to acid, and the effect of applied external energy (ultrasonic). The main focus was to optimize the conditions needed for production of transparent gel of NCCs. In the efforts to increase the transparency of nanocrystals, the ultrasonic energy was applied on the course of the reaction or after the reaction to break down the aggregates and to further promote the efficiency of acid hydrolysis. While the application of ultrasonic energy after hydrolysis has been previously documented [1], but the mechanism of ultrasonic effect has not been clearly understood till today. Due to the cellulose's strong ability to form hydrogen bonds, the produced nanocrystals tended to agglomerate to form larger particles. The aggregate formation manifested itself especially in the absence of surface charges when the repulsion forces between the individual nanocrystals were minimized. One solution for decreasing the aggregation issue is to introduce negative charges on the surface of CNCs. Sulfuric acid is known to introduce negative charges on the surface of the CNCs via an esterification reaction with the sulfate anions [2-4].

It has been proved that the complete hydrolysis of cellulose under strong acid and high temperature (~100^{o}C) results in glucose or even carbonization [5, 6]. While under relatively mild conditions in the present study, the chemical degradation mechanism can be acid-catalyzed cleavage of β-1-4-glycosidic bond [7]. The degradation of MCC could proceed in three steps, outline shown in Fig.4.1. Firstly, the glycosidic oxygen linking two sugar units is rapidly protonated under acidic condition, forming a conjugate acid. Then the cleavage of the C–O bond and breakdown of the conjugate acid to the carbonium ion take place. After a rapid addition of water, the resulted segments and a proton are liberated. Assuming that the cleavage of the C–O bond takes place more rapidly at the end than in the middle of the polysaccharide chain, more monosaccharides and lower yields of NCC are resulted.

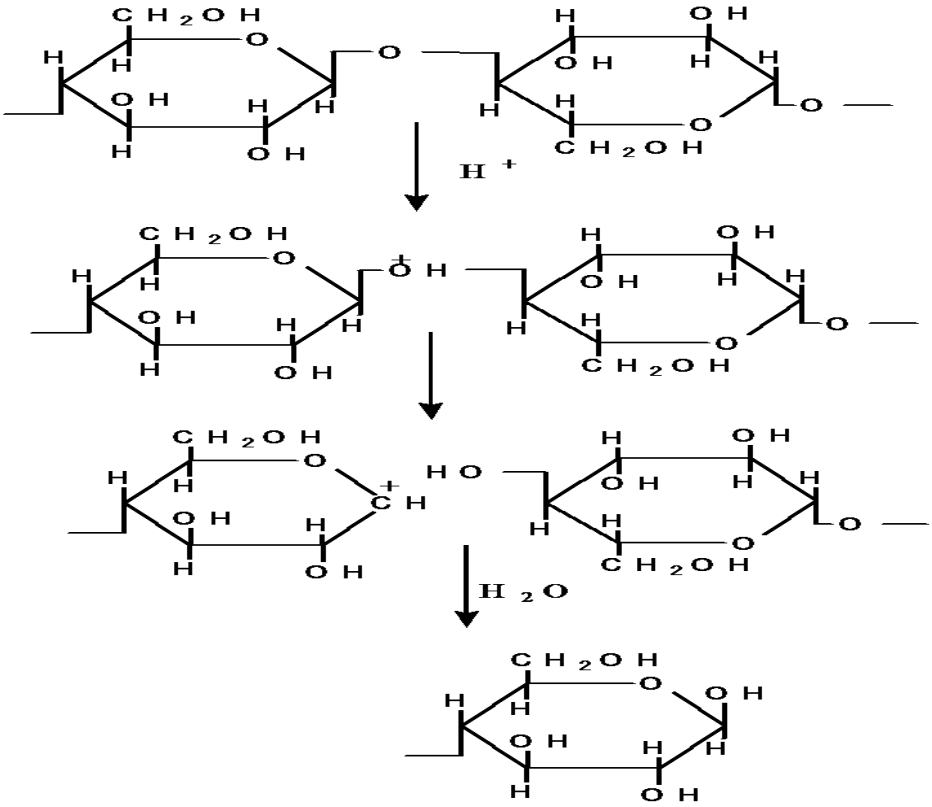

Fig. 4.1: Mechanism of acid-catalyzed hydrolysis of MCC by cleavage of β-1-4- glycosidic bond

4.2 Characterization of NCC prepared through H_2SO_4 hydrolysis

A complete set of experiments were performed to examine the formation of transparent NCC without complete hydrolysis. The acid concentration less than 60% gave white powder like as starting MCC. On the other hand acid concentration more than 70% gave blackish product; it may be due the carbonization of cellulose. These finding gave us an indication to choose 64% sulfuric acid concentration for hydrolysis purpose and at this concentration the product formed look like almost transparent gel [1]. At the same way acid to MCC ratio, temperature of the hydrolysis and time for hydrolysis were also investigated and the results from those study gave indication to choose the optimum condition for hydrolysis. The optimum condition [8] of hydrolysis was carried out at 60 ^{o}C temperature for 90 minutes with 64% (w/w) H_2SO_4 at the acid to MCC ratio 20: 1.

After hydrolysis the diameter and size of fibrils of hydrolyzed cellulose was reduced to great extent due to removal of most the amorphous region of microcrystalline cellulose leaving nano-scale cross-linked fiber like crystals. Fig. 4.2(a) shows the FESEM micrographs of a very dilute suspension of NCC, showing agglomerated 'cross-linked fiber' nanocrystals. The diameter of nanocrystals has wide range of distribution but the size of most of the 'cross-linked fiber' nanocrystals lies within the range 100-300 nm in length and 10-20 nm in diameter shown in FESEM in Fig.4.2 (b). Their compact agglomeration of CNCs shows that cellulose chains have an intermolecular hydrogen bonding and a strong hydrophilic interaction in between the cellulosic chains. From Fig. 4.2(c), the FESEM image of starting MCC, it can say that MCC particles were irregular shapes and their average diameter was about 10 μm and length was about 50 μm. The irregularity may be due to the presence more amorphous region in MCC compare to NCC. From the above discussion it can be claimed that microcrystalline cellulose is successfully converted into nanocrystalline cellulose.

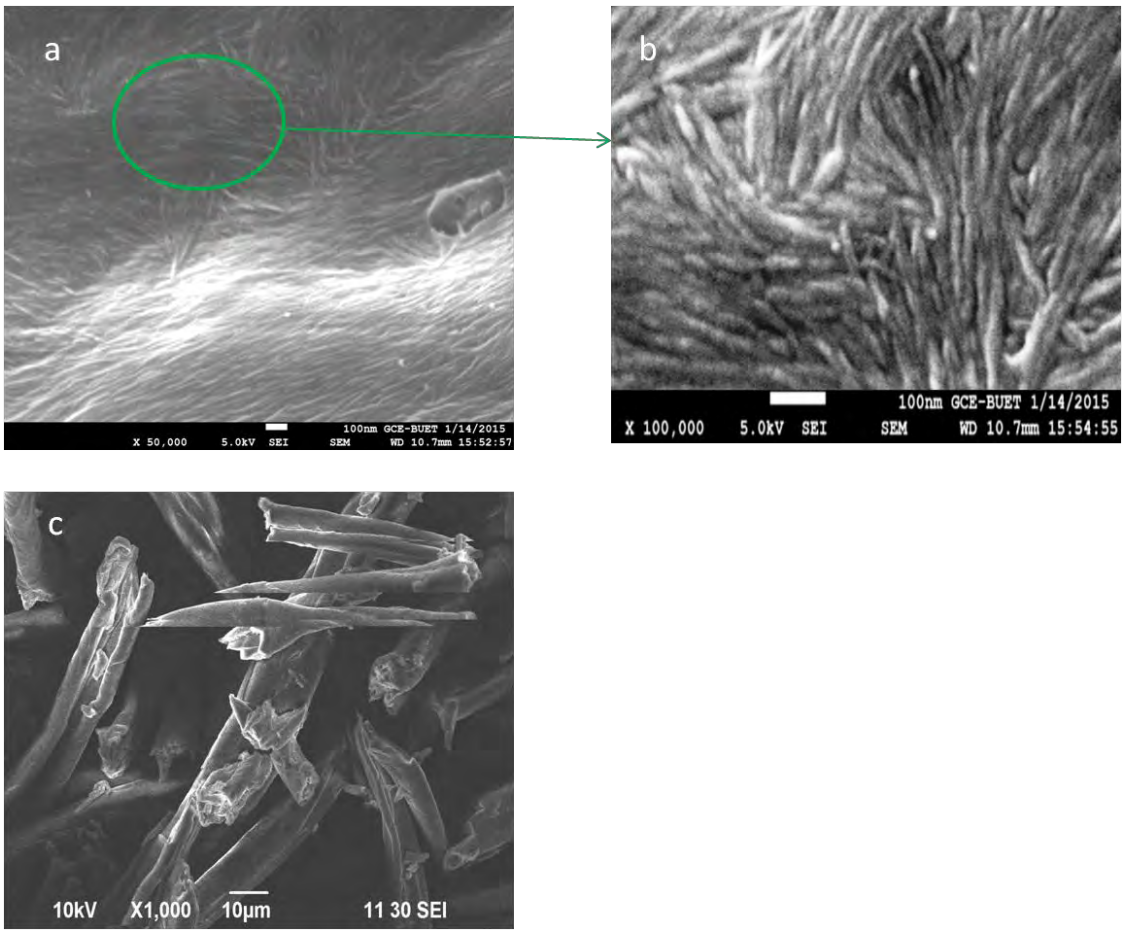

Fig 4.2: (a) and (b) FESEM image of NCC and (c) FESEM image of NCC

4.3 Characterization of NCC prepared through HCl hydrolysis

Fig. 4.3 shows the FESEM micrograph of NCC prepared through hydrochloric acid hydrolysis from MCC. It is clear that the 6 M HCl acid also produced 'cross-linked fiber' crystallites however, which are in micro-scale with a diameter 100 to 200 nm and length 1 to 10 μm. This result indicates that the crystallites are almost transformed to nano-sclae. So, it can be assumed that if the hydrochloric acid concentration, reaction time and temperature to be maintained with proper condition MCC would be converted into NCC.

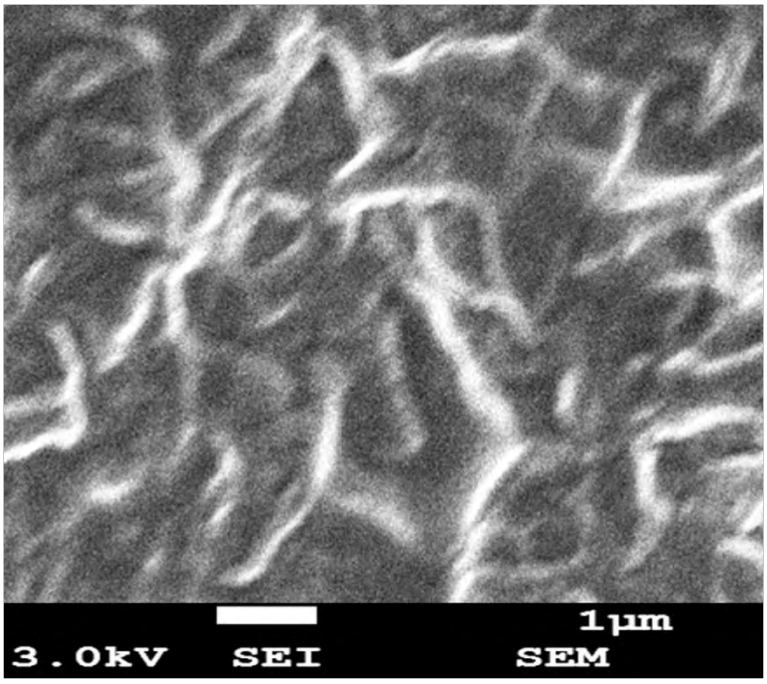

Fig.4.3: FESEM micrograph of NCC through HCl acid hydrolysis of MCC

4.4 Characterization of NCC prepared through mixture of H_2SO_4 and HCl hydrolysis

In case of the mixture of acids the hydrolysis condition seems milder than H_2SO_4 or HCl acid hydrolysis. It took longer hydrolysis time (8 hours) to produce transparent NCC gel. The shape and size of the NCCs were investigated by FESEM. In contrast with sulfuric acid hydrolysis that produces 'cross-linked fiber' cellulose nanocrystals but the mixture acids gave spherical nanoparticle with larger size. The FESEM image shown in Fig.4.4 is that of NCC particles obtained from mixture acid were spherical in shape with an average diameter less than 100 nm.

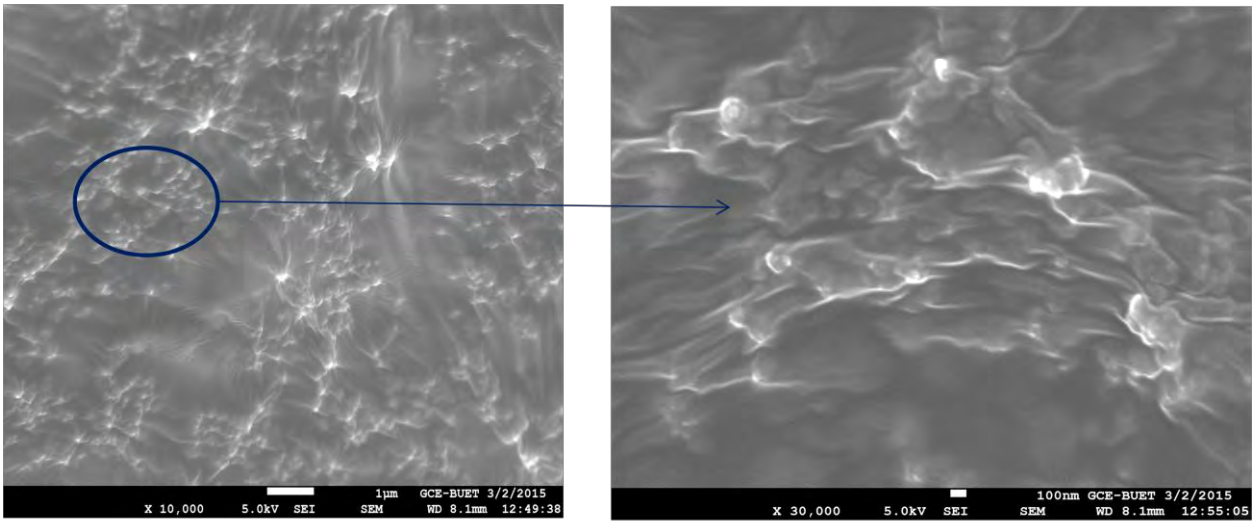

Fig. 4.4: FESEM image of spherical NCC prepared through mixture of H_2SO_4 acid & HCl acid

4.5 Characterization functionalized nanocellulose

4.5.1 Characterization of dialdehyde nanocellulose

Periodate oxidation is known to be a highly specific reaction to convert 1, 2-dihydroxyl groups (glycol) to paired aldehyde groups without significant side reactions [9, 10]. During the oxidation, 1 mol of NCC theoretically consumes 1mol of $NaIO_4$ [11]. The degree of oxidation, which corresponds with the aldehyde content (AC), is generally determined by measuring the amount of reactive aldehydes available for oxime formation, or from copper titration. Since cellulose is polymer, only surface hydroxyl groups will react with the oxidant and 100 % conversion is not possible. In this study it was found that about 42% conversion of vicinal hydroxyl groups to dialdehyde group through copper titration and oxime formation method. This oxidation is temperature sensitive and increasing temperature is favorable for the periodate oxidization at the beginning due to the nature of the endothermic reaction. However, if the reaction temperature is higher than 55 ^oC, decomposition of periodate will predominate thus the effect of the oxidant will lost more or less. That's why 48 ^oC temperature was chosen for the periodate oxidation. The presence of dialdehydic group was

confirmed from the FTIR spectra (Fig. 4.5) and ^{1}HNMR (Fig. 4.6) spectra as well as by the classical functional group test with hydrazine reagent gave orange precipitate (Fig.4.7).

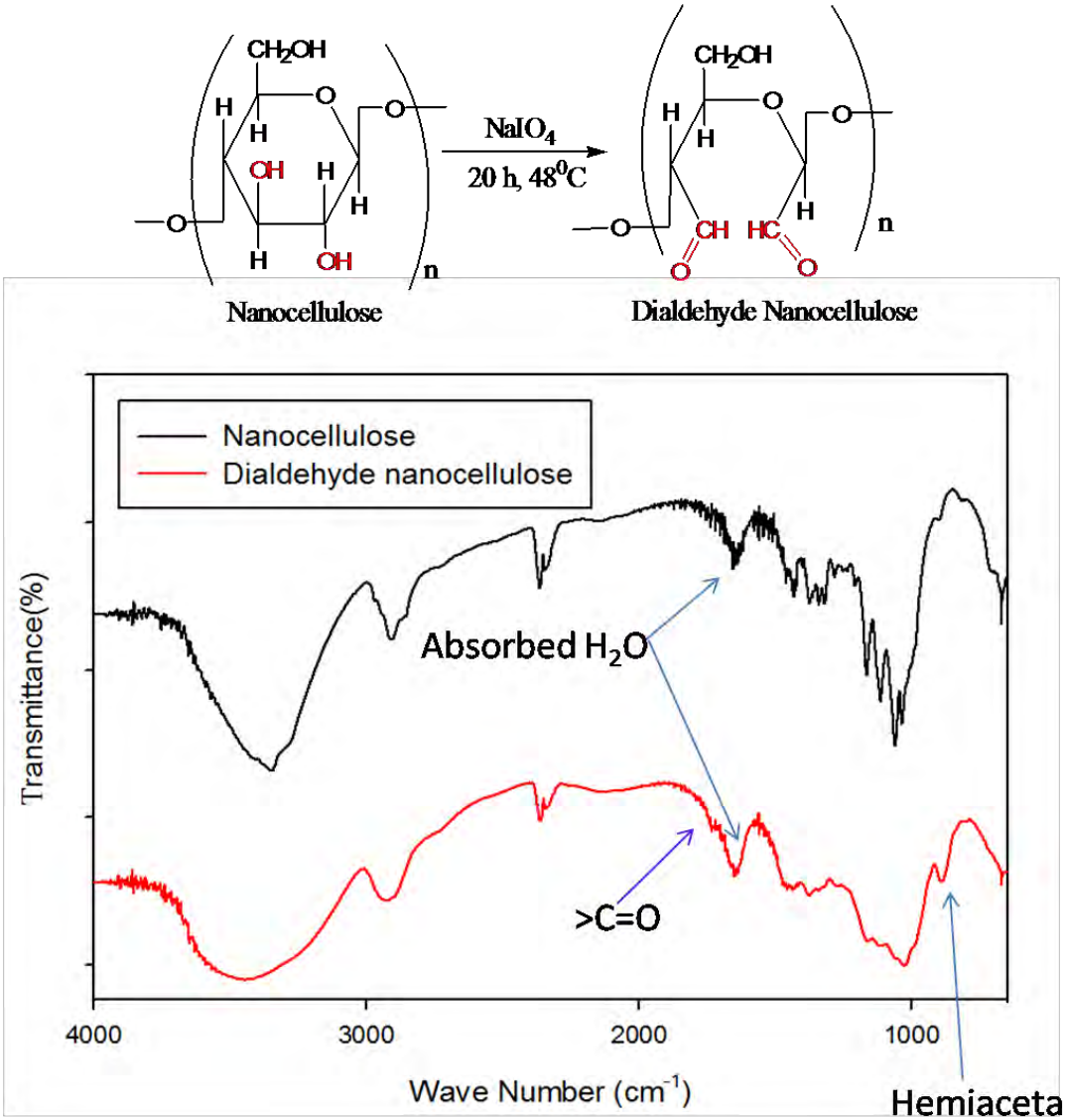

Fig. 4.5: FTIR spectra of Nanocellulose and Dialdehyde nanocellulose

The FTIR spectra of prepared nanocrystalline cellulose and periodate oxidized dialdehyde nanocellulose (DANC) are shown in Fig. 4.5. The broad peak near about at 3400 cm^{-1} is due to the stretching of –OH groups, the peak at 1300 cm^{-1} due to the –OH bending vibration[12]; the peaks at 2900 cm^{-1}, 1430cm^{-1} and1020 cm^{-1} are assigned to -C-H stretching vibration, -CH_2 scissoring and -CH_2-O-CH_2- stretching, respectively [13]. It is clear that two characteristic IR bands at ~1738 cm^{-1} (very weak) and 890 cm^{-1} regions appear in oxidized NCC. Even though high degrees of oxidation can be obtained by periodate oxidation, the carbonyl groups can hardly be detected by spectroscopic methods such as FTIR spectroscopy

[14], likely due to hydration and acetalization effects. Severe drying down to 7% relative humidity and high temperatures eventually increased the C = O vibrations [15, 16], which indicated a large extent of hydration of the carbonyl groups in these substrates. Other explanations are strong cross-linking by the formation of hemicaetals with neighboring hydroxyl groups. As cellulose have both reducing end and non-reducing end and the reducing end can form a hemiacetal bond from adlehydic group and adjacent hydroxyl group.

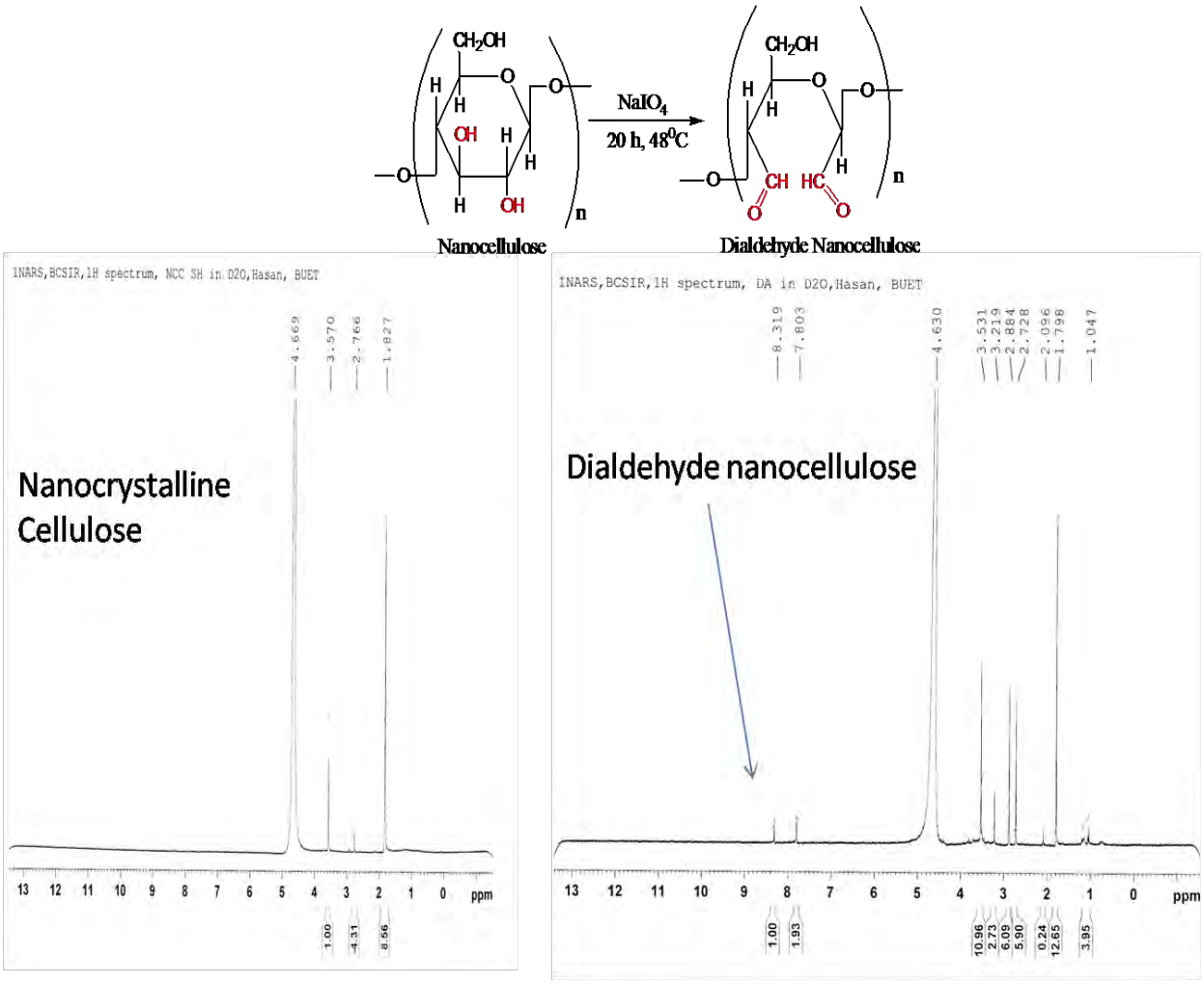

Fig. 4.6: ^{1}HNMR spectra of Nanocrystalline cellulose and dialdehyde nanocellulose

That's why NCC always shows a weak peak at ~890 cm^{-1} but during oxidation the intensity of that peak increased because of there are more available aldehyde groups to form hemiacetal bonds with neighboring hydroxyl groups. Which is consistent with the reported FTIR spectra of periodate oxidized cellulose [14, 11, 17]. Generally, the peak at about 1740 cm^{-1} is characteristic of aldehydic carbonyl groups, while the band around 890 cm^{-1} is assigned to the formation of hemiacetal bonds between the aldehyde groups and neighbor

hydroxyl groups. The results indicate that the aldehyde group has been introduced into the structure by selective periodate oxidation of NCC.

The dialdehyde formation was further confirmed by ^{1}HNMR spectra of NCC and DANC (fig. 4.6). The two signals at δ_H7.803 ppm and δ_H 8.319 ppm are assignable two aldehydic protons of dialdehyde nanocellulose and other signals within the 1.0 -5.0 ppm might be due to the oxymethine, oxymetylene and hydroxyl protons of cellulose.

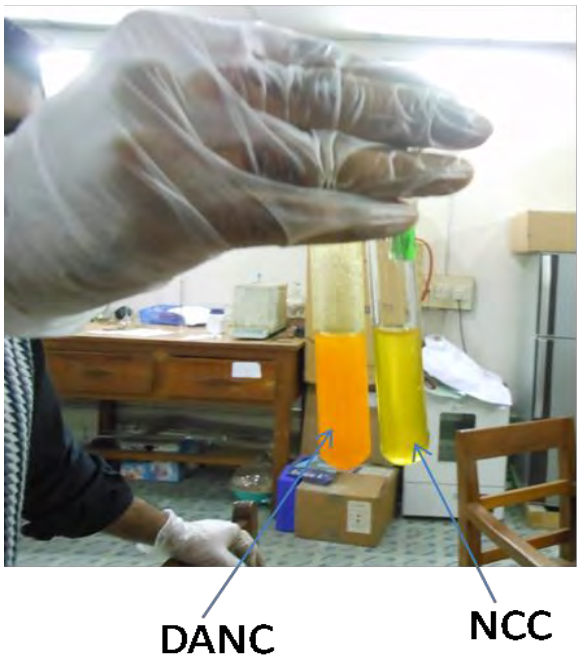

Fig.4.7: Hydrazine test for carbonyl group detection of dialdehyde nanocellulose

4.5.2 Characterization of dicarboxylated and tri-hydroxyl nanocellulose

The functionality of the chlorite-oxidized dicarboxylated cellulose was confirmed by the disappearance of the aldehyde bands at 1730 cm^{-1} and weakening of the intensity of hemiacetal signal at 890 cm^{-1} and the appearance of new band at1650 cm^{-1} in FTIR spectra (Fig. 4.8). These new band is associated with dissociated forms of carboxyl groups, which indicate the formation of dicarboxyl-containing celluloses which was further confirmed by the disappearance of two dialdehyde signals in ^{1}HNMR (Fig.4.9) spectra of dicarboxylated nanocellulose.

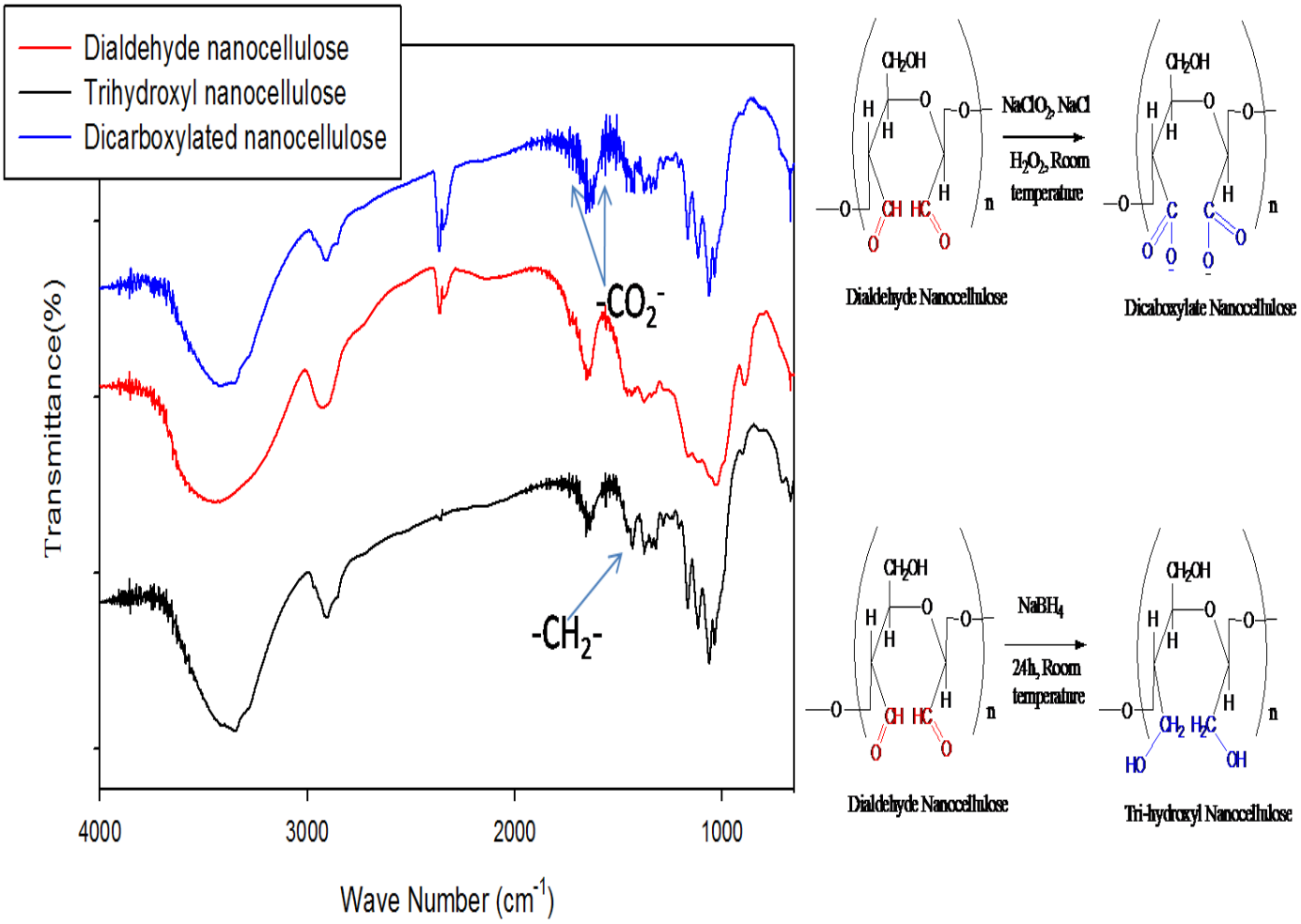

Fig. 4.8: FTIR spectra of NCC, Dicarboxylated NCC and Tri-hydroxyl NCC

The functionality of $NaBH_4$ reduced tri-hydroxyl cellulose was also confirmed by the disappearance of the aldehyde bands at 1730 cm^{-1} and weakening of the intensity of hemiacetal signal at 890 cm^{-1} and strengthening the peak at 1425 cm^{-1} in FTIR spectra (Fig.4.8) due the increasing number hydroxyl groups in the cellulose chain. This observation was further confirmed by the almost diminishing of two aldehydic signals in ^{1}HNMR (Fig.4.9) spectra during reduction. A weak signal at δ_H 7.803 ppm indicates that one of the aldehydic protons may not be 100% converted into alcohol. The conversion of aldehyde groups to acid groups and alcohol groups also confirmed by the negative test with hydrazine reagent (Fig.4.10).

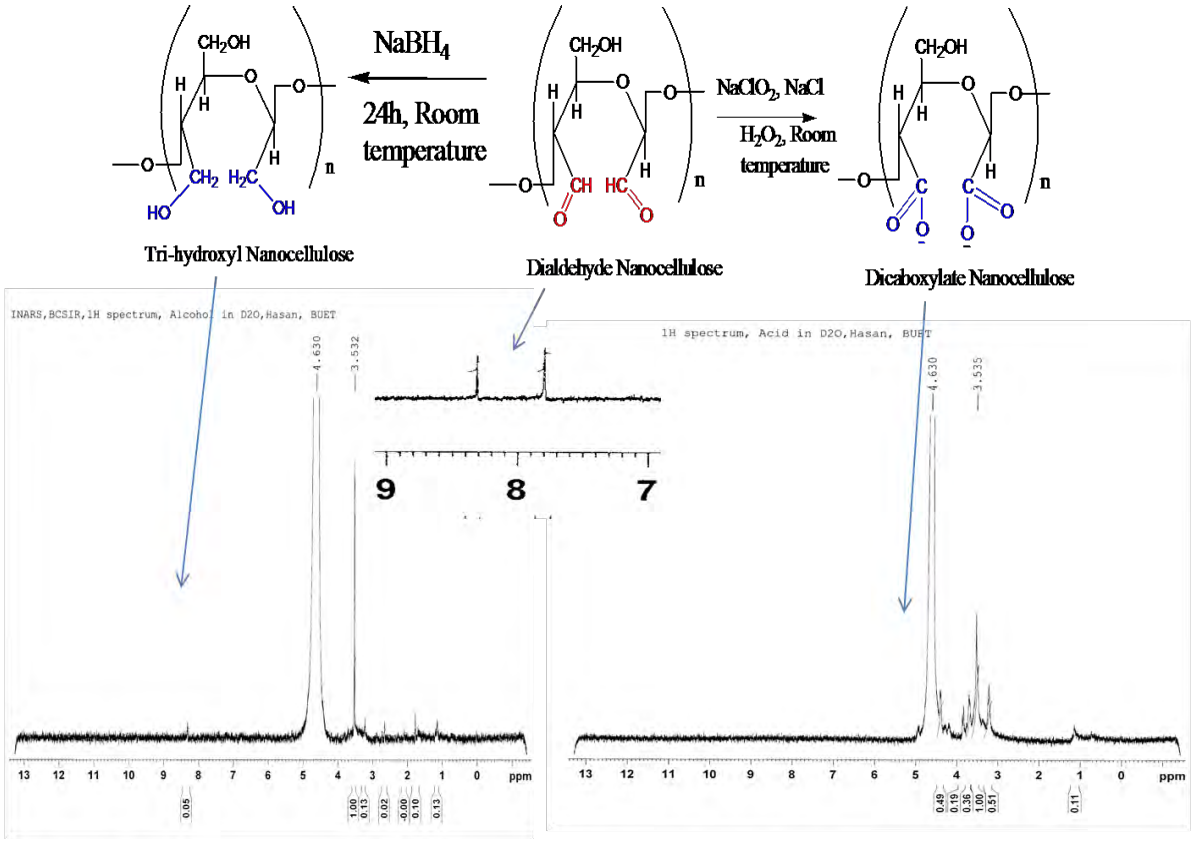

Fig. 4.9: ^{1}H NMR spectra of NCC, Dicarboxylated NCC and Tri-hydroxyl NCC

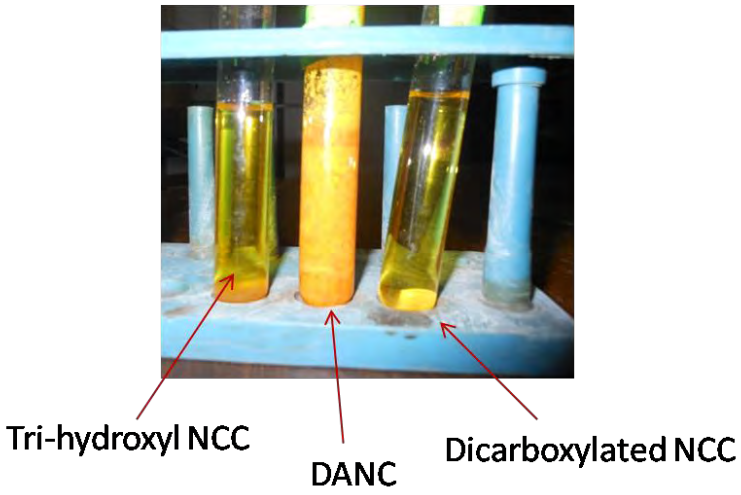

Fig.4.10: Hydrazine test for carbonyl group confirmation of DANC, Dicarboxylated NCC and Tri-hydroxyl NCC

4.6 Characterization of Schiff's base derivative

4.6.1 Characterization of Schiff's base derivative prepared from aliphatic primary amine

Dialdehyde nanocellulose was converted into stable secondary amine derivatives with ethylene diamine and hydroxyl amine hydrochloride via reductive amination method. The secondary amine derivatives were characterized by FTIR spectra with compare to starting dialdehyde nanocellulose. The spectra showed a new band near ~1510 cm^{-1} [18] for secondary amine (-N-H bending) group (Fig. 4.11) while the carbonyl band of aldehyde groups at 1730 cm^{-1} was almost disappeared. The disappearance of the carbonyl stretching band is due to the formation of carbon-nitrogen bond between the dialdehyde cellulose and amine bearing precursor molecule. Moreover, the intensity of hemiacetal band at ~890cm^{-1} decreased during amination which also indicate the conversion of aldehydic group into amine group.

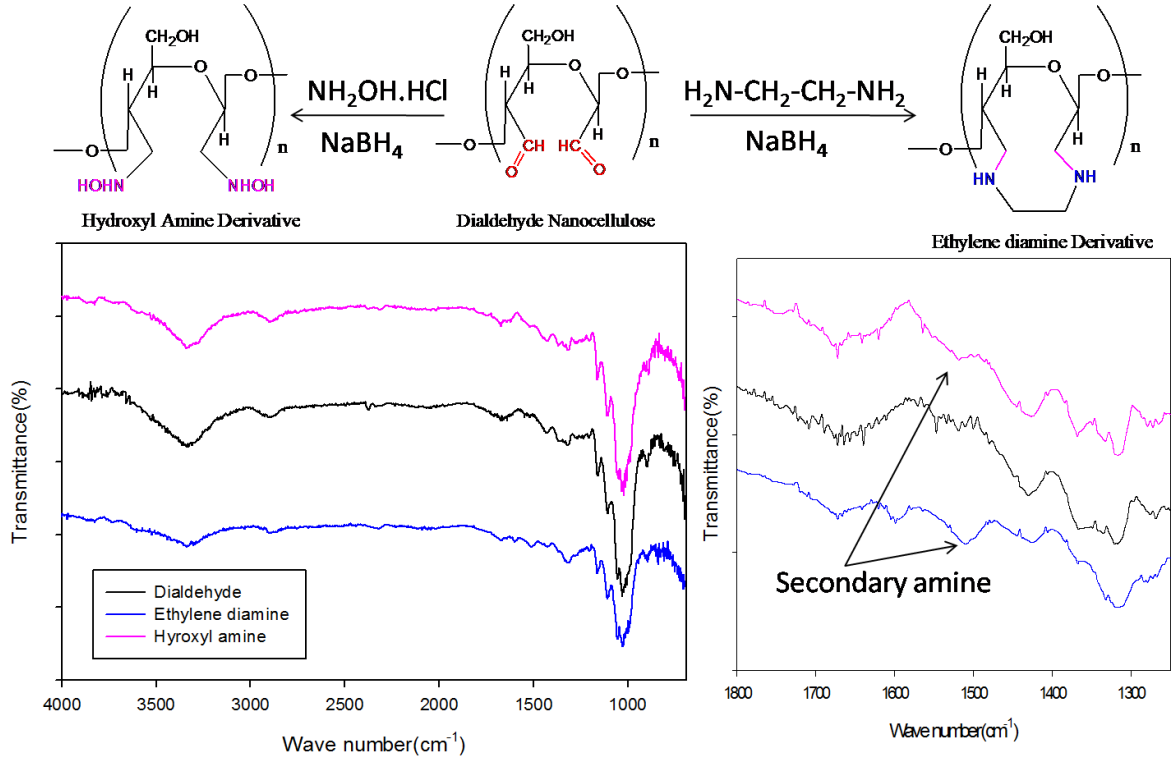

Fig. 4.11: FTIR spectra of Dialdehyde Nanocellulose, Hydroxyl amine derivative and Ethylene diamine derivative

4.6.2 Characterization of Schiff's base derivative prepared from aniline and 4-nitroaniline

The prepared dialdehyde cellulose was reacted with aniline and 4-nitroaniline to generate *in situ* the corresponding imines (Schiff's base) followed by sodium borohydride reduction to yield the stable secondary amine derivatives. The presence of the secondary amine functionality in derivatized nanocellulose was evidenced from FTIR spectra (Fig.4.12) as indicated by the appearance of a new band at 1,510 cm^{-1} corresponding to N–H bending vibration. The appearance of new band at ~1600 cm^{-1} is characteristic of aromatic –C-H bond which was originated from aromatic precursor molecules. It also can clearly be seen from the FTIR spectra that after the reaction the intensities of the characteristic hemiacetal band at ~890 cm^{-1} decreased approximately 80% when compared dialdehyde. A new band at ~850 cm^{-1} further confirms the incorporation of aromatic group into the cellulose unit.

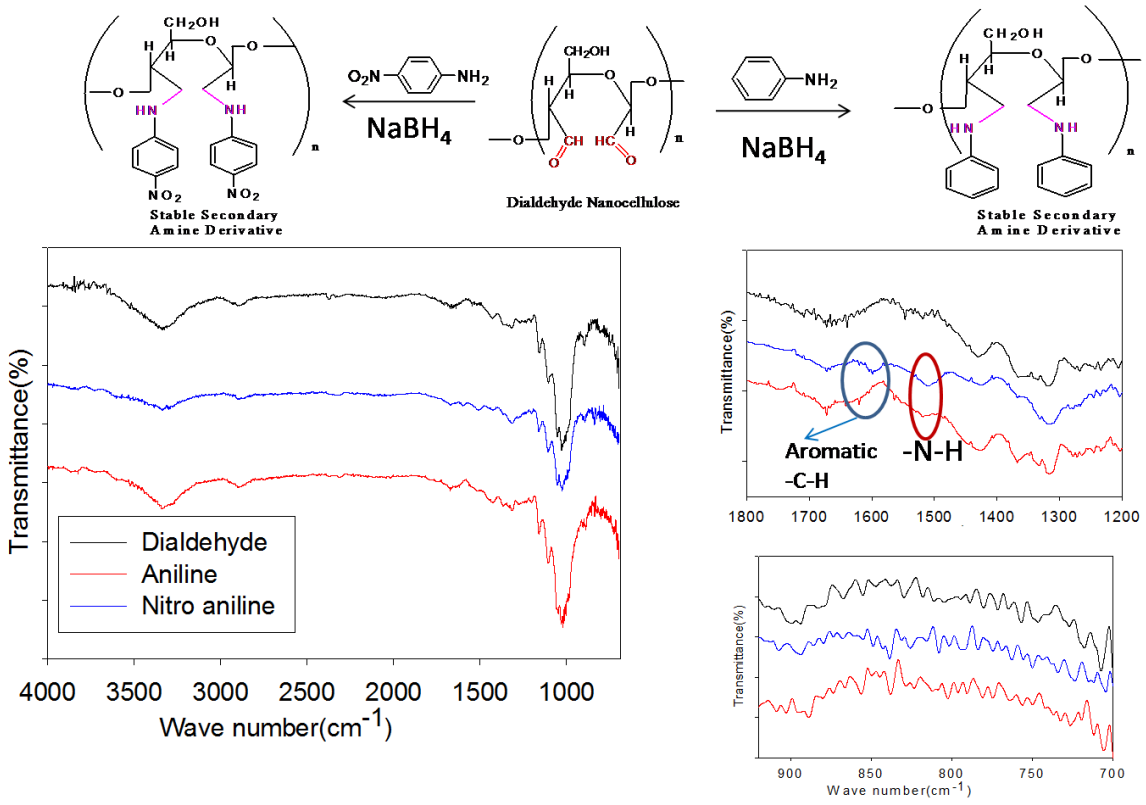

Fig. 4.12: FTIR spectra of Dialdehyde Nanocellulose, aniline and p-nitroaniline derivative

4.6.3 Characterization of Schiff's base derivative from p-hydroxyaniline

Formation Schiff's base derivative of p-hydroxyaniline with dialdehyde was confirmed by FTIR spectra (Fig.4.13) and proton NMR (Fig.4.14) spectra. A new band at 1520 cm^{-1} is confirmative for –N-H bending vibration of secondary amine group of prepared derivative. Moreover, a tiny peak ~3300 cm^{-1} which is absent in dialdehyde cellulose with a strong hydroxyl peak also confirm the conversion. Again the intensity of hemiacetal band at ~890 cm^{-1} decreased during amination which also indicate the conversion of aldehydic group into amine group. This observation was further confirmed by the weakening of two aldehydic signals in ^{1}HNMR spectra during reduction and appearance of new signal at δ_H 6.8 ppm which is due to the incorporation of aromatic ring in cellulose chain. The weakening of the two aldehydic signals indicates that the aldehydic protons may not be 100% converted into amine.

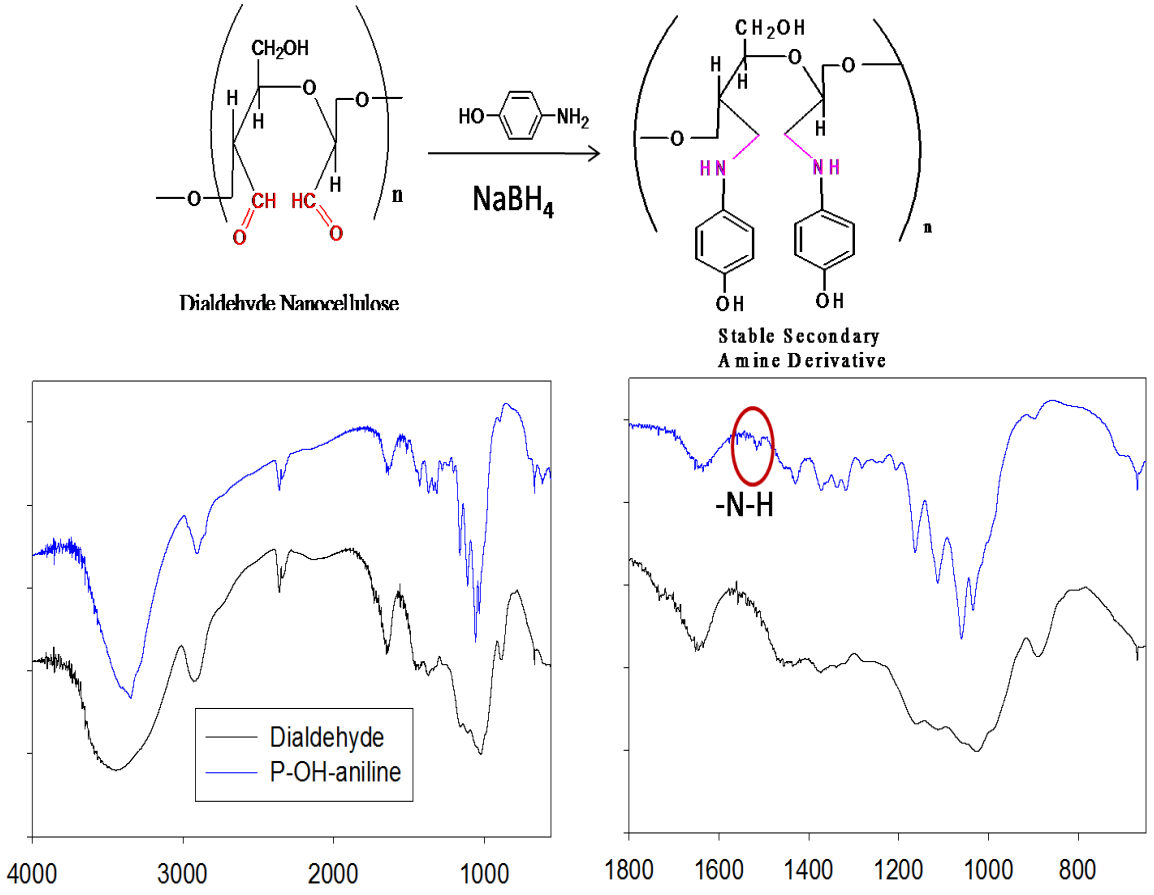

Fig.4.13: FTIR spectra of Dialdehyde Nanocellulose and stable secondary amine derivative of p-hydroxyaniline

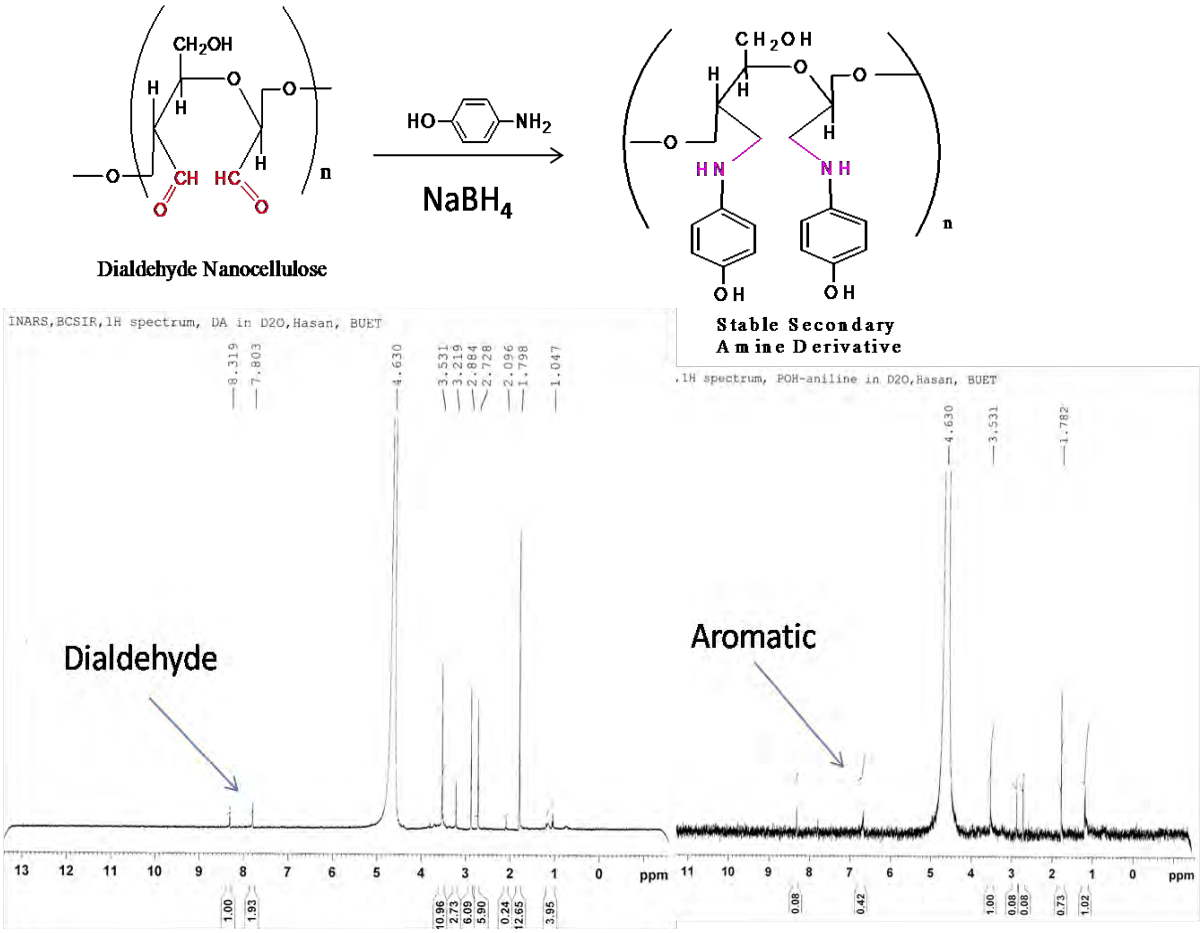

Fig.4.14: [1]HNMR spectra of dialdehyde nanocellulose and stable secondary amine derivative of p-hydroxyaniline

4.7 Physical appearance, Surface morphology and Crystallites sizes

Fig.4.15 shows NCC at different conditions. The appearance of a stable glossy gel at the concentration of 4% NCC is an obvious indication of the presence of NCC. The NCC powder is obtained by freeze drying exhibits white metallic luster color. Vacuum evaporation of aqueous suspensions of NCC at room temperature produces solid films with perfect optical transparency. Figure 4.16 shows the physical appearance of NCC and functionalized NCC in aqueous suspension and glossy gel state. All functionalized NCC have almost similar physical appearance with slight variation of transparency. This slight variation of appearance might be due to the different crystallites size and hydrogen bonding in functionalized NCC.

Fig.4.17 shows aqueous suspension and thin film of aromatic primary amine derivative of NCC. All amine derivatized NCC shows color-suspension and film which might be due to the incorporation of aromatic amine group into NCC chain.

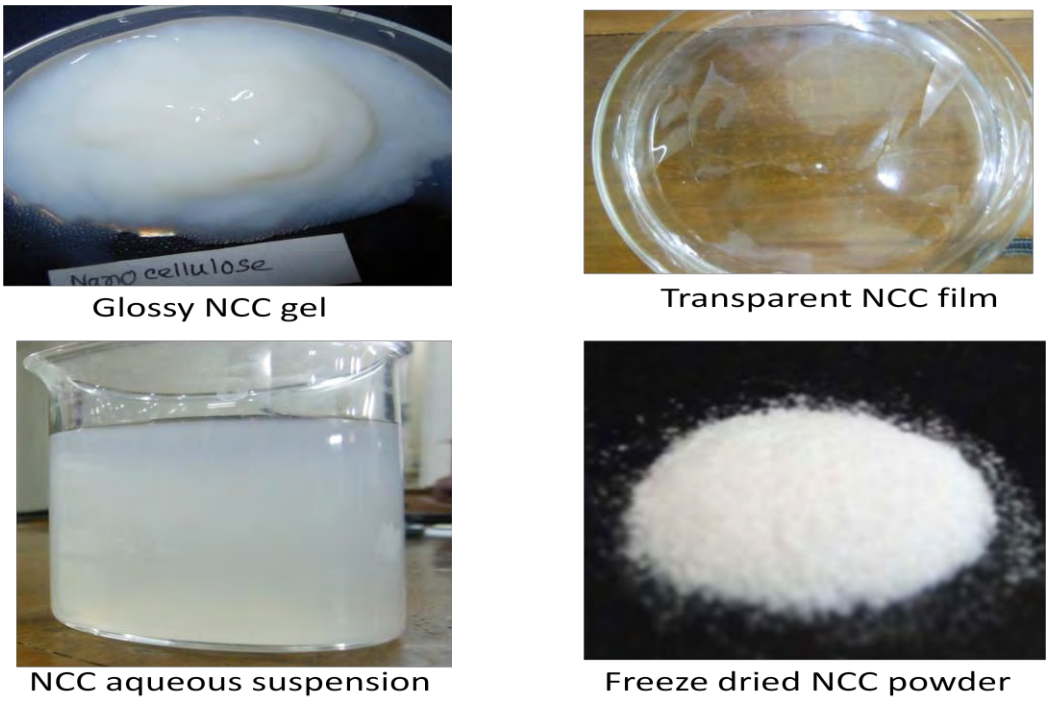

Fig. 4.15: Physical appearance of NCC at different conditions

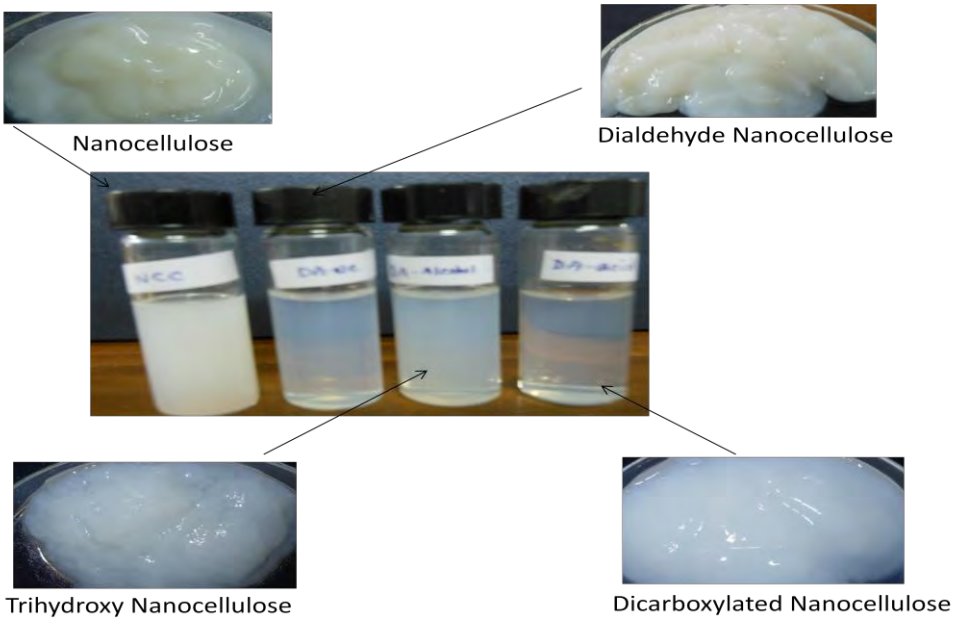

Fig.4.16: Physical appearance of NCC and functionalized NCC in gel state and in aqueous suspension state

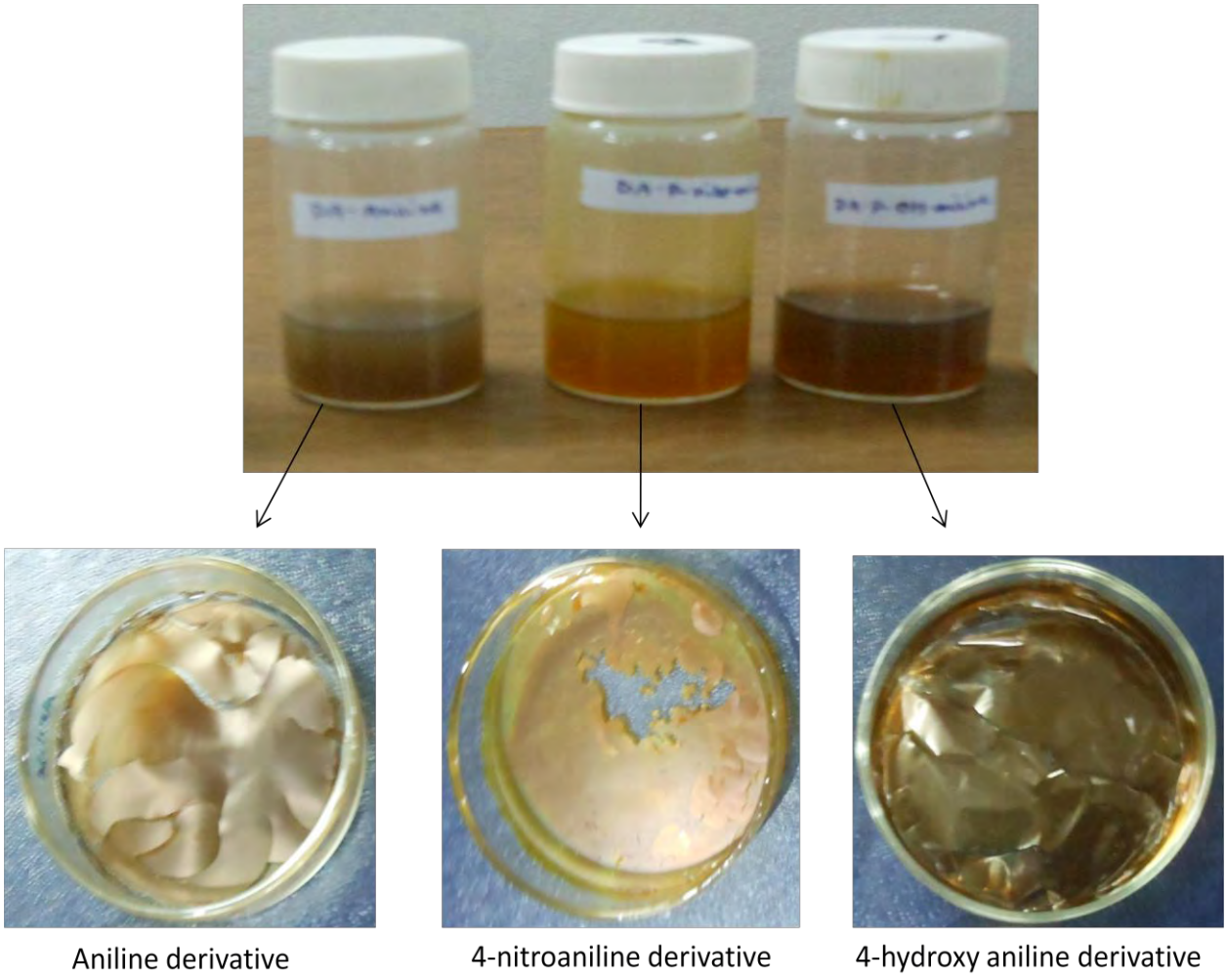

Fig.4.17: Physical appearance of aqueous suspension and thin film of aromatic amine derivative of NCC

Investigation of surface morphology of functionalized nanocrystalline cellulose, and its derivatives was carried out by FESEM as shown in Fig. 4.18. After periodate oxidation the fiber diameter decreased, it can be assumed that periodate might have some degree of hydrolysis capacity along with its oxidizing capacity. However, during chlorite oxidation the fiber dispersibility increased compare to that of the NCC and DANC. This was probably due to the carboxyl content introduced during the oxidation, which consequently increased the electrostatic repulsion between the cellulose chains. On the other hand SEM images of derivatized NCC show that the all derivatized NCC maintained their characteristic morphology even after grafting with amines. The starting dialdehyde cellulose seems to be

agglomerated before chemical modifications but they were found to be separated from each other after chemical modification. This may be due to the incorporation of relatively hydrophobic groups on the surface.

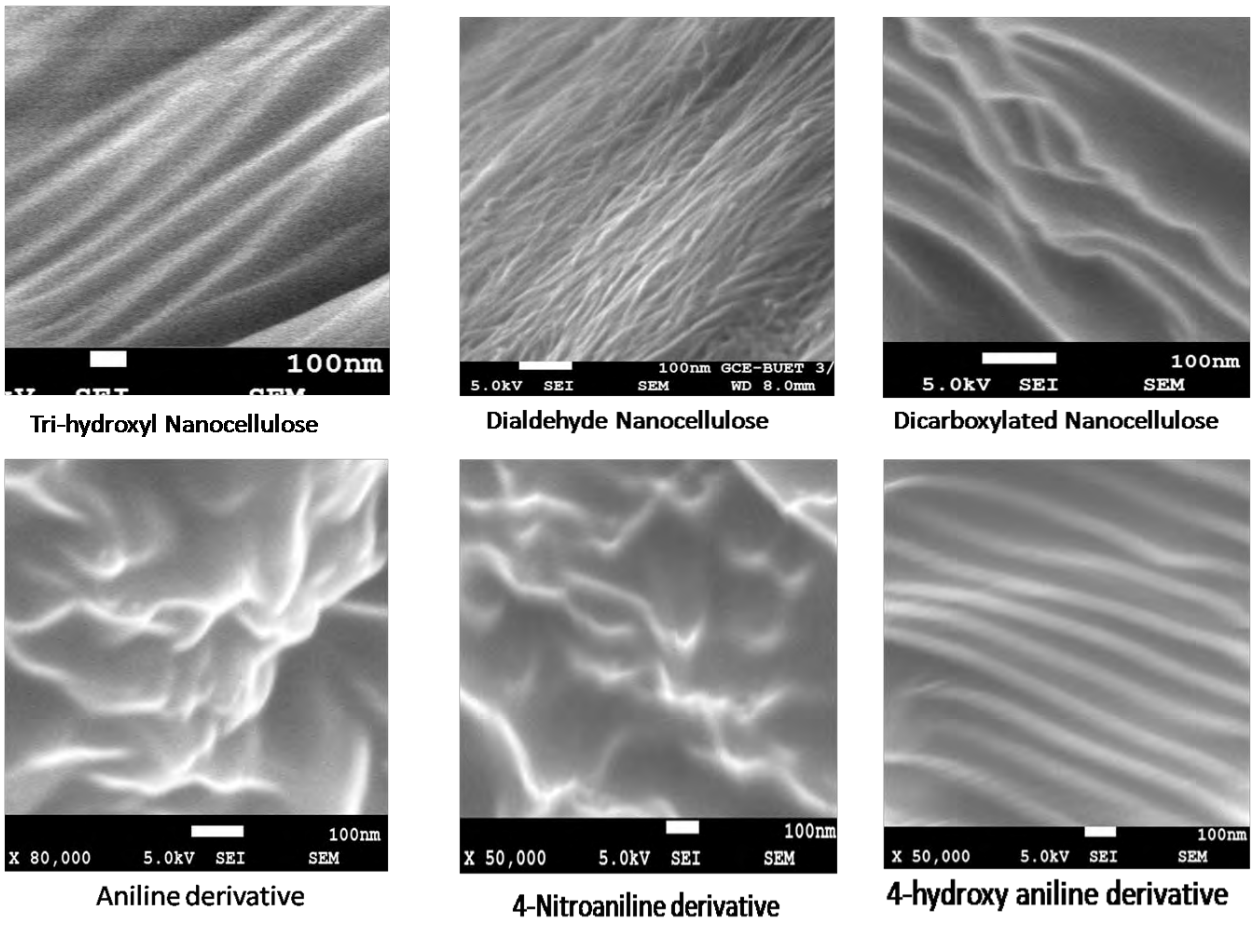

Fig.4.18: FESEM images of functionalized and derivatized NCCs

So, from the above FESEM images it can be concluded that all the functionalized and derivatized NCCs have in nano-scale dimension with some morphological differences.

4.8 X-ray diffraction (XRD) Analysis

The effect of the oxidations on the crystal structure of cellulose was measured using XRD. The XRD profiles of starting nanocellulose and modified nanocellulose are presented in Fig.4.19. All the samples exhibited a peak around $2\theta = 16.5^{o}$ and 22.5^{o} and 34.6^{o} which are supposed to represent the typical cellulose structure. The cellulose crystals exhibit characteristic assignments of 110, 200, and 004 planes, respectively [19-22]. The NCC and other modified NCC have similar characteristic peaks at the same position. The only difference that is discernible is slight change in their peak intensities, representing some changes in the crystallinity during modification of cellulose. This is consistent with the previously reported results [23] and indicates that no rearrangement of the cellulose structure into another crystalline form occurred.

The crystallinity index of the samples was calculated according to amorphous subtraction method. The crystallinity index (C.I.) of cellulose is defined as [24]:

$$\text{Crystallinity index} = \frac{I_{002} - I_{am}}{I_{002}} \quad \text{----------} \quad (4.1)$$

Here, I_{200} is the intensity of the 200 planes reflection, typically located around $2\theta = 22.5^{0}$; I_{AM} is the intensity at $2\theta = 18^{0}$, corresponding to the minimum in a diffractogram [25].

Using Eq. (4.1), the C.I. of the starting nanocrystalline cellulose was 91.24 %, whereas the C.I. was decreased to 88.14 % for the Dialdehyde nanocellulose, 87.97 % for tri-hydroxyl nanocellulose, 75.00 % for dicarboxylated nanocellulose and 86.00 % for p-hydroxy aniline derivative of Dialdehyde nanocellulose. This result is consistent with the experiments performed by Kim et al. (2000), who found that the crystalline index of cellulose was decreased according to the oxidation level by periodate and chlorite [17]. The loss of crystallinity is considered to result from opening of glucopyranose rings and destruction of their ordered packing [11]

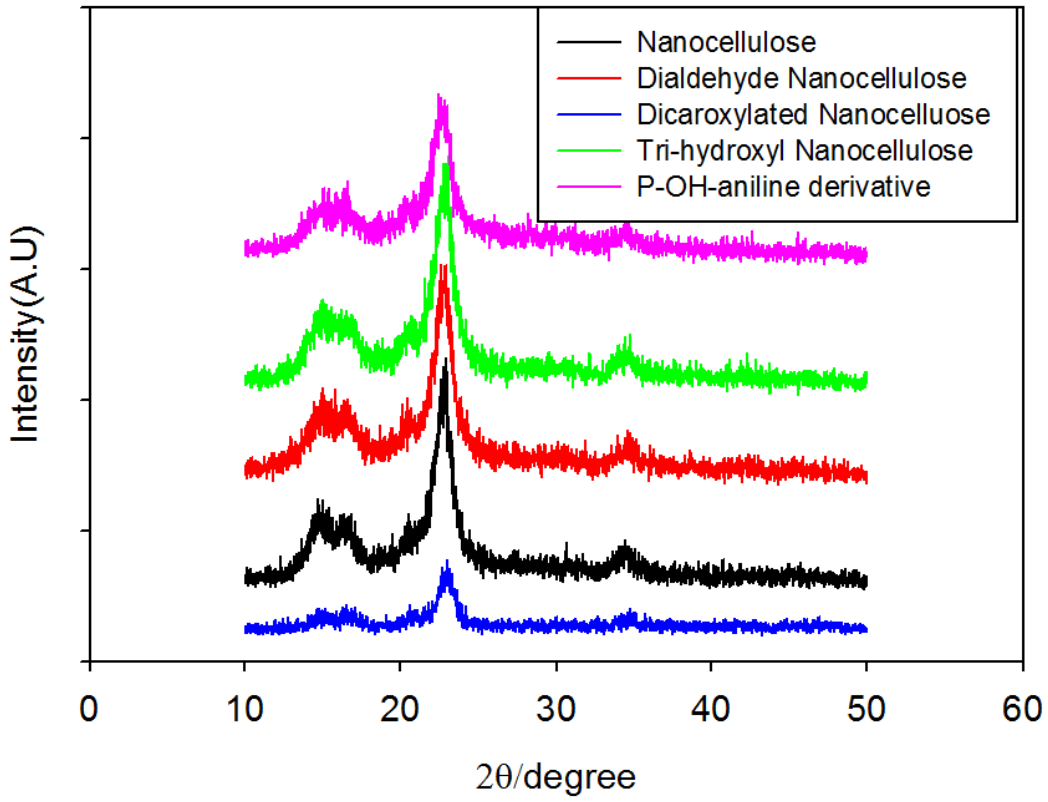

Fig.4.19: Comparison of XRD data of NCC functionalized NCC and derivatized NCC

Table 4.1: Crystallinity index of NCC, functionalized and derivatized NCC

Samples	Crystallinity Index (C.I.)
Nanocrystalline cellulose	91.24 %
Dialdehyde nanocellulose	88.14 %
Dicarboxylated nanocellulose	75.00 %
Trihydroxyl nanocellulose	87.97 %
4-hydroxy aniline derivative	86.00 %

The calculated crystalline indexes decreased during periodate oxidation and chlorite oxidation, this decrease has been assumed to be due to cellulose chain degradation and changes in the hydrogen bonding. Therefore, it can be assumed the oxidation reactions were

not fully restricted to surfaces of crystalline surfaces and also affected the core of crystallinities. It was observed that CrI was preserved even after the reductive amination reaction, which could be due to the grafting of small molecules onto the cellulose chain. This observation confirms that the crystalline core of the cellulose chain is not affected by the coupling and reduction reaction, which is therefore limited only to the surfaces. Similar observation was made in the literature, where morphology and crystallinity of NCC is retained after chemical modification [26].

4.9 Thermo-degradation behavior of NCC and functionalized NCC

Thermal analysis techniques such as thermogravimetry (TG), derivative thermogravimetry (DTG) and differential thermal analysis (DTA) were widely used to measure the thermal stability and pyrolysis behavior of polymers in different conditions. TG curves show only changes in weight during heating and its derivative shows changes in the TG slope which may not be obvious from the curve of TG. The DTA curves show the difference in temperature as exothermic or endothermic reactions in a sample. The results of the thermogravimetric (TG) analysis of NCC and other functionalized NCCs are shown in fig. 4.20 and differential thermogravimetric (DTG) and differential thermal analysis (DTA) of one of the (tri-hydroxyl alcohol) functionalized NCCs is shown in fig.4.21 for find out the actual thermal behavior of the materials. All samples showed a slight weight loss at low temperatures (< 150^0C), corresponding to evaporation of absorbed water. However, the degradation behavior was different in the high temperature range. The starting MCC showed one major pyrolysis process but acid-hydrolyzed CNCs and modified NCCS showed mainly two humps or shoulder in close proximity where lower degradation temperature may correspond to highly sulfated amorphous regions and higher degradation temperature correspond to unsulfated part of the material [27]. All samples showed one major pyrolysis process, and associated weight loss in the temperature range from 230 to 340^0 C was observed but the maximum weight loss occurred at different temperature from one another which might be due to the changing of functional group in glucose unit of cellulose chain. The first weight loss occurred at 220-340^0 C of NCC and functional NCCs which was caused by the molecular motion of amorphous regions and thermal scission of covalent bonds, which led to the generation of volatile substances [28,29]. At high temperatures, the depolymerization pathway of cellulose yields tar (levoglucosan), which further decomposes with the formation of char and this mostly occurs in crystalline regions. Generally, cellulose

thermal degradation involves dehydration, depolymerisation and decomposition of glycosyl-units and then formation of a charred residue. In case of CNC and other modified NCCs, thermal degradation occurs at a lower temperature within broader ranges of temperature showing lower thermal stability due to their nano-sizes, greater number of free ends in the chain of CNCs, and may show drastic reduction in the molecular weight and degradation of highly sulfated amorphous regions [30].]. Here, remnant sulfate groups are responsible for the reduced thermal-stability of the nanocrystals [27] because the elimination of H_2SO_4 in sulfated anhydro-glucose units require less energy [31], therefore, sulfuric acid molecules were released at much lower temperatures during the degradation process.

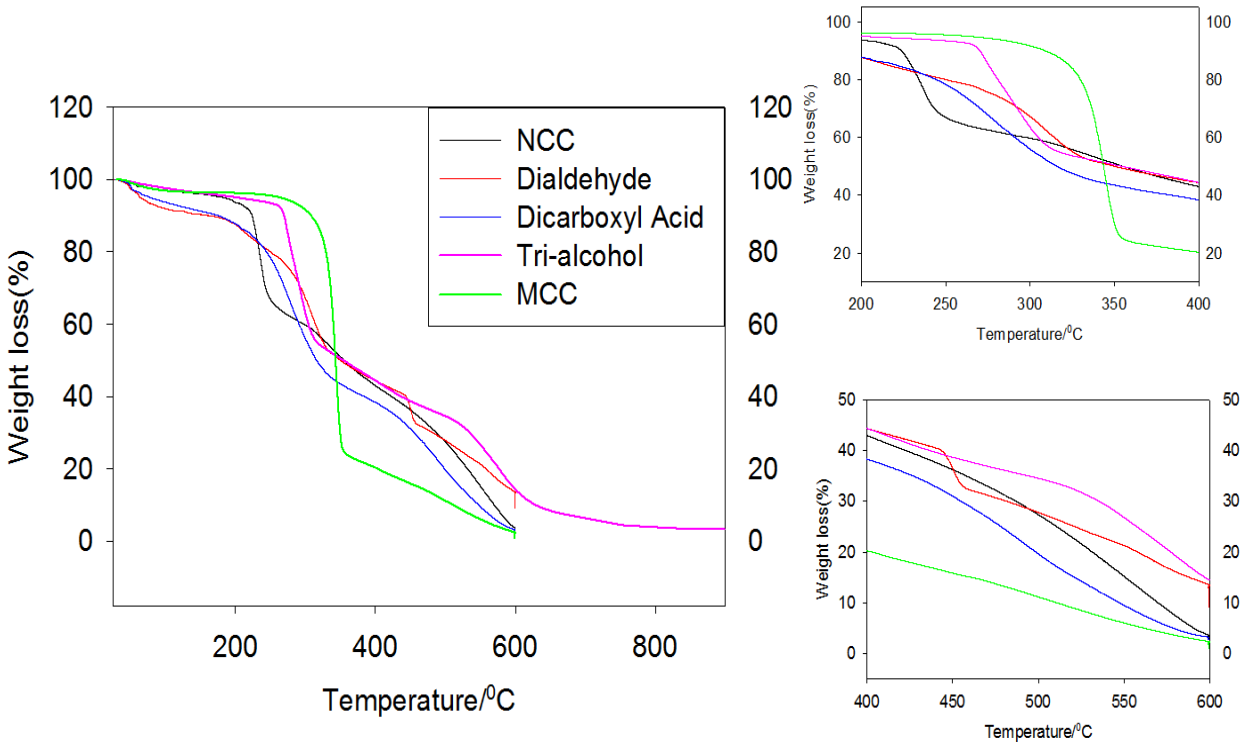

Fig. 4.20: Comparison of thermogravimetry (TG) curves of NCC and other functionalized NCCs

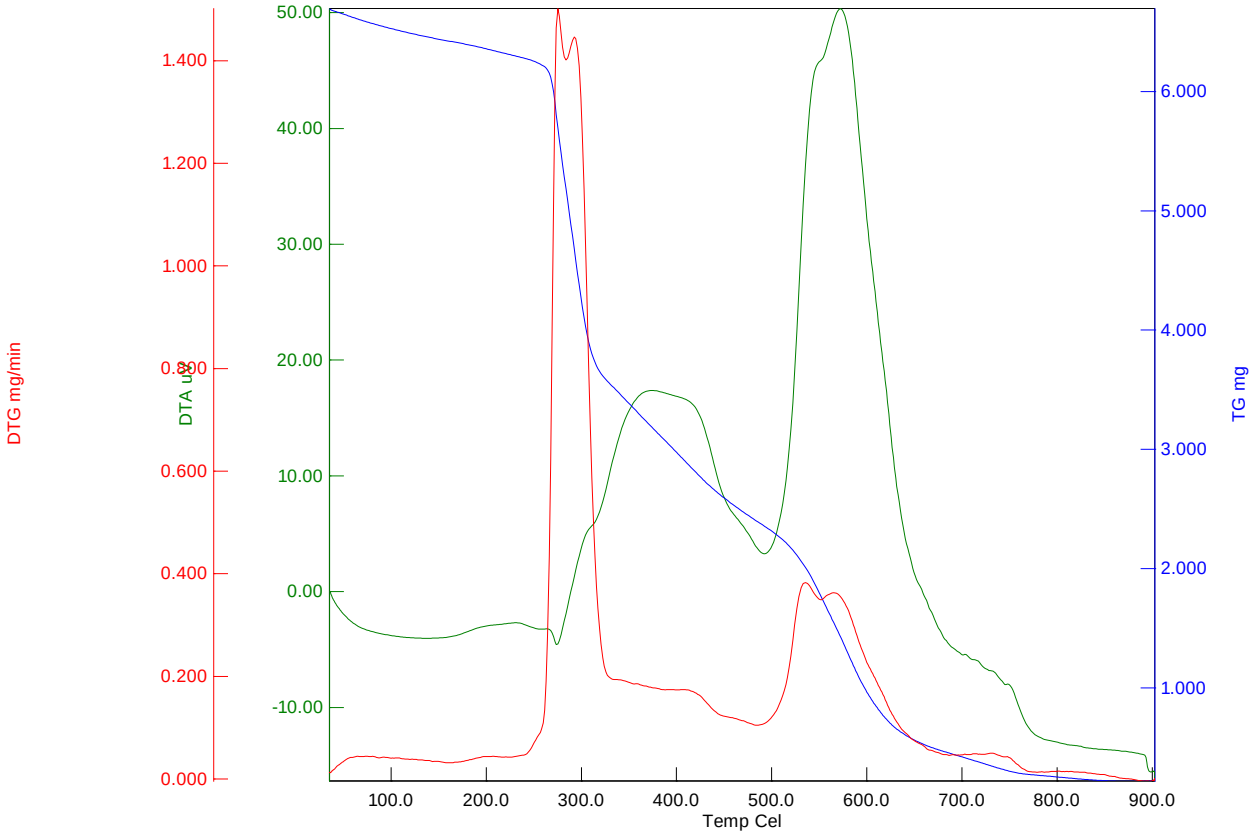

Fig. 4.21: TG, DTG and DTA curves of Tri-hydroxyl nanocellulose

The initial and final degradation temperature (IDT and FDT) and maximum degradation temperature (*T*max), were tabulated in Table 4.2. The initial weight loss started at 50 °C for all samples, and was attributed to the evaporation of the moisture in the fibers. After 370 °C, the entire organic compound presented in the fibers degraded, black carbonaceous residue (inorganic compound), known as char, remained. As shown in Table 4.2, the initial degradation temperature of NCC, functionalized NCCs and derivatized NCCs decreasing from MCC, indicated that the modified were less thermally stable than MCC. Although the crystallinity of NCC and modified NCCs is higher compare to MCC, the maximum degradation temperature was found to be lower (Table 4.2). The probable cause was that the large amounts of hydroxyl groups exposed with the increased specific surface areas were absorbing atmospheric moisture; and along with the rising temperature, sulfate ester bonds

desorbed and reacted with the water molecules to create sulfuric acid, leading to structural damage to NCC and a reduction in the thermal degradation temperature[32].

Table 4.2: IDT, FDT and Tmax of NCC and modified NCC

Sample	IDT	FDT	T_{max}
Microcrystalline cellulose	315 (12.5%)	354(75.4%)	334
Nanocrystalline cellulose	220 (9.5%)	250 (23.3%)	236
Dialdehyde Nanocellulose	270 (23.5%)	325(45.4%)	312
Tri-hydroxyl Nanocellulose	265 (8.3%)	312 (45.5%)	280
Dicarboxylated Nanocellulose	240 (19.80%)	320 (50.5%)	282
Hydroxyl amine Derivative	250 (13.5%)	310 (45%)	283
Aniline Derivative	275 (10.12%)	370 (42%)	312
4-nitroaniline Derivative	265 (12.2%)	325 (50.3%)	298
4-hydoxyaniline Derivative	290 (8.50%)	360 (57.7%)	330

DTA traces of one of the functionalized and one of the derivatized NCCs show one distinct endothermic change and one exothermic change (as shown in Fig.4.21 and 4.23). Endothermic change occurs at lower 300 °C due to thermal scission of covalent bonds. Exothermic changes at around 530-540 ^{o}C may be due to the depolymerization of glucose unit from crystalline region and char formation occur. In case of acid-hydrolyzed CNCs, all amorphous regions were dissolved and only nano-scale cellulose crystals having sulfated hydroxyl (-OH) groups and gives higher onset temperature of crystal melting with wider endotherm width in turn (220-350 °C). After the reactions between the DANC and primary amines, the first-step weight loss also decreased and the second-step weight loss remain almost same with slight variation. The DTG curves of amine derivative showed the first peak temperature increased with compare to NCC. It may be due the effect of cross linking reaction between oxidized cellulose and amines which restricted the molecular chain mobility of derivative NCCs, so the thermal stability increased.

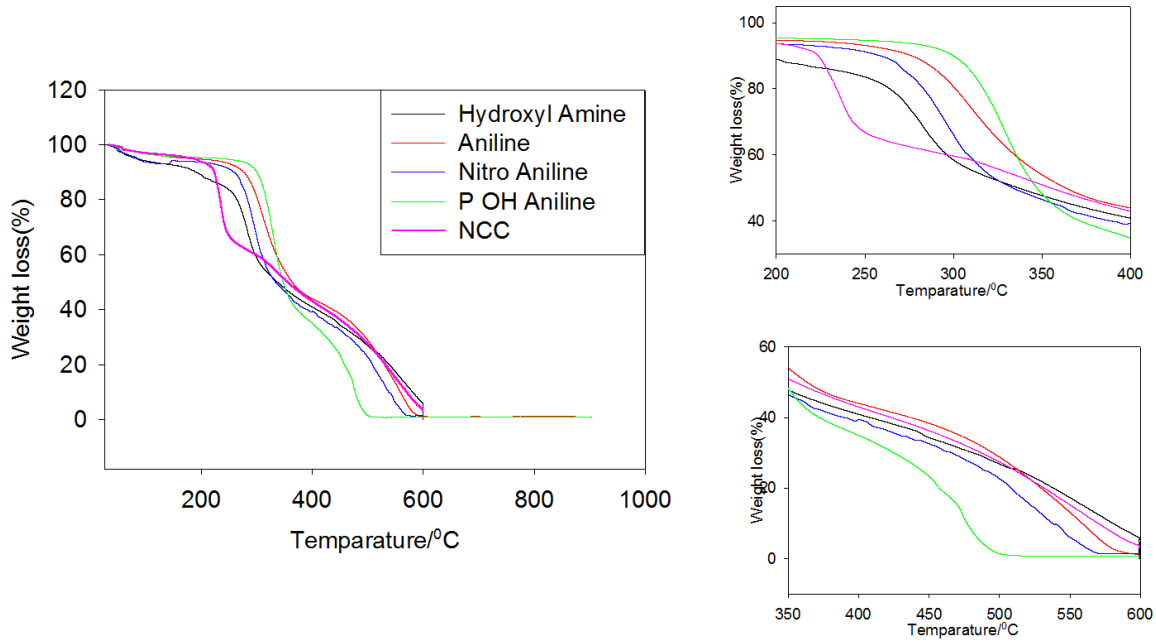

Fig.4.22: Comparison of thermogravimetry (TG) curves of NCC and other amine derivatized NCCs

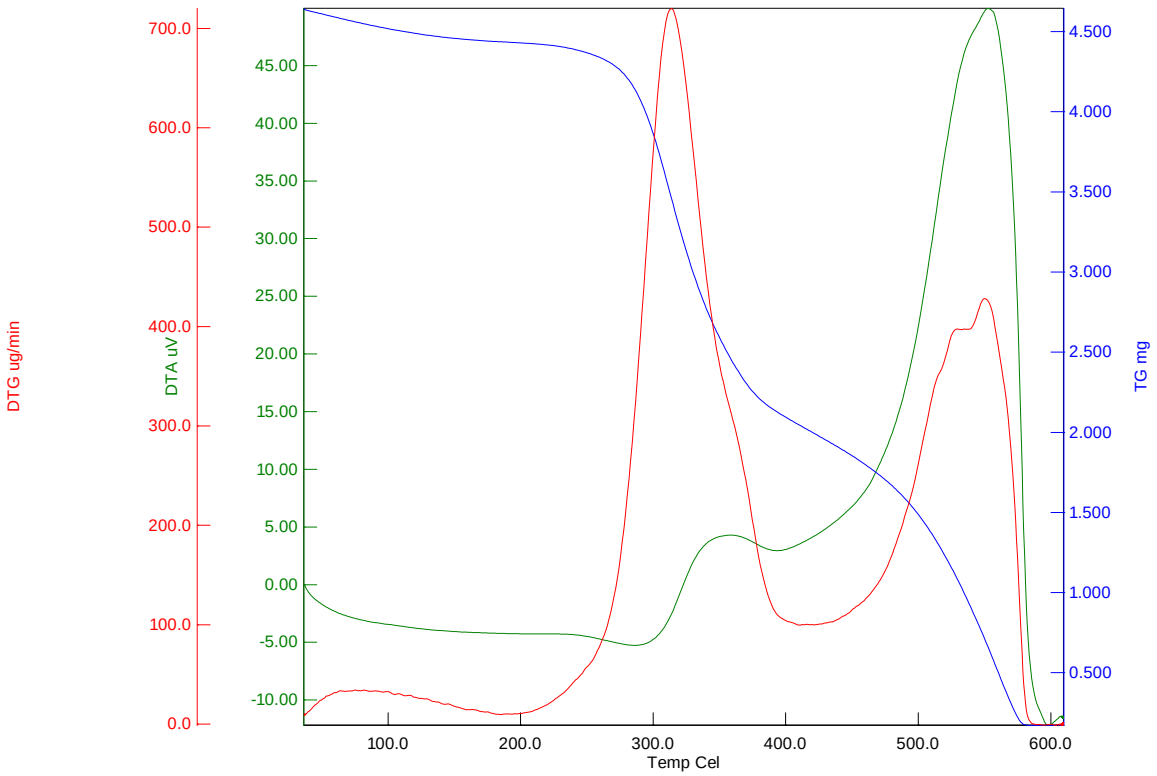

Fig. 4.23: TG, DTG and DTA curves of aniline derivative of nanocellulose

4.10 Surface Charge behavior NCC and it functionalized NCC

Point of zero charge (pzc) for a given sample is the pH at which that surface has a net neutral charge. Sulfuric acid is known to introduce negative charges on the surface of the CNCs via an esterification reaction with the sulfate anions. This negative surface charge can be verified by determining the point of zero charge of NCC and other functionalized materials. From table 4.3 and the expanded portion of fig.4.24 it is clear that NCC and all functionalized NCC have negative surface charge as the point of zero charge of all samples are less than seven. NCC and other functionalized NCC showed a slight variation of point of zero charge. NCC showed at 4.98 pH and it selective oxidized dialdehyde product showed at 5.43 pH. This result suggest that during sulfuric acid hydrolysis negative surface charge derived from sulfatation of surface hydroxyl groups in glucose unit while during periodate oxidation this sulfate ester groups desorbed and amount negative charge on surface has been reduced. On the other hand dicarboxylated nanocellulose showed point of zero charge at 4.92 pH. This more negative surface charge can be explained as during chlorite oxidation two negatively charged carboxylated groups introduced in every glucose unit of cellulose chain.

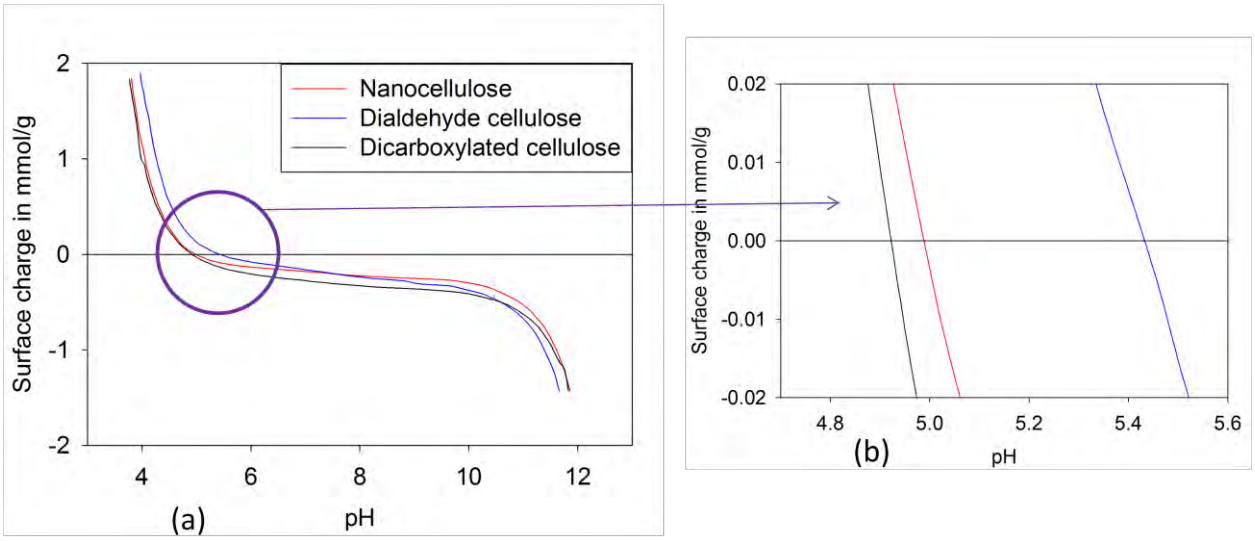

Fig. 4.24: Surface charge comparison of NCC and functionalized NCC

Table 3.3: Point of zero charge of NCC and functionalized NCC

Sample	Point of zero charge(pH)
Nanocrystalline cellulose	4.98
Dialdehyde nanocellulose	5.10
Dicarboxylated nanocellulose	4.92

The significance of Point of zero charge is that a given sample surface will have positive charge at solution pH values less than the pzc and thus be a surface on which anions may adsorb. On the other hand, that sample surface will have negative charge at solution pH values greater than the pzc and thus be a surface on which cations may adsorb. So, prepared NCC and it functionalized materials can be used as positive charge adsorber at neutral solution or basic solution or even negatively charge substance can adsorbed at low pH than pzc of the sample. This property can be used for controlled drug delivery purpose at different pH condition.

4.11 Transparency studies of NCC and modified NCC

Aqueous slurry of microcrystalline cellulose on class slide form a non transparent white thin layer but nanocellulose and other modified nanocellulose form a transparent thin film (Fig. 4.25). Both slides were kept on a small piece of paper which was written NCC and MCC and figure bellow clearly shows NCC is transparent whereas MCC is not.

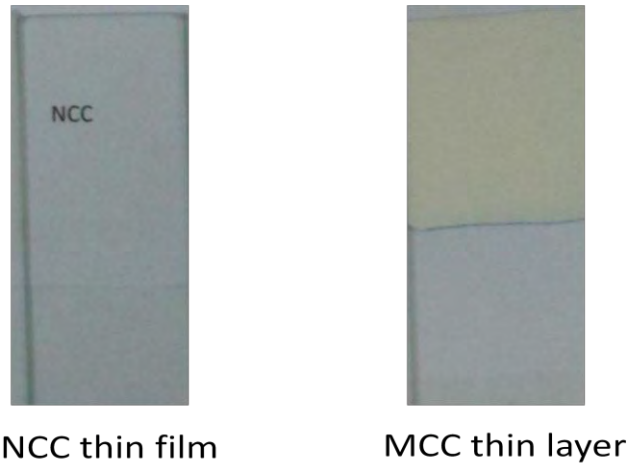

Fig. 4.25: Thin layer of NCC and MCC on glass slide

Fig.4.26, Fig.4.27 and Table 4.4 showed the comparison of transparency of nanocrystalline cellulose and other modified nanocellulose materials thin film at visible region. Nanocellulose has lowest transparency than other modified nanocellulose. As nanocellulose is the starting material for dialdehyde functionalization and dialdehyde is the starting material for other functionalized or derivatized materials. During periodate oxidation of nanocellulose, the individual fiber diameter decreased and this may be the cause of increased transparency of dialdehyde product and other modified materials. When Schiff's base derivatives were prepared with small primary aliphatic amines, transparency remain almost constant with slight variation but when those were prepared with aromatic amines, the transparency decreased abruptly. These may be due to the small molecules of primary aliphatic amines grafted on cellulose fiber having not affected much but with larger aromatic amines the grafted effect may be prominent. However, an exception is seen with 4-hydroxyaniline this decreased value might be due to the introducing of polar hydroxyl groups into the cellulose chain. During chlorite oxidation and borohydride reduction of dialdehyde cellulose, the transparency again decreased these might be due to the introducing of polar carboxylate groups and hydroxyl groups into the cellulose chain respectively. Which may be formed a large number of hydrogen bonds with neighboring chain.

Table 4.4: Transmittance of nanocrystalline cellulose and modified nanocellulose at visible region.

Sample	Transmittance at 800 nm (%)	Transmittance at 600 nm (%)	Transmittance at 350 nm (%)
Nanocrystalline cellulose	48.51	41.79	29.60
Dialdehyde nanocellulose	83.45	79.77	35.71
Dicarboxylated nanocellulose	74.85	66.05	30.80
Tri-hydroxyl nanocellulose	57.88	51.77	7.88
Hydroxyl amine derivative	87.80	81.54	40.02
Ethylene diamine derivative	80.94	79.45	72.17
Aniline derivative	51.17	42.25	29.14
4-nitroaniline derivative	57.71	38.40	20.90
4-hydroxyaniline derivative	81.82	54.17	19.02

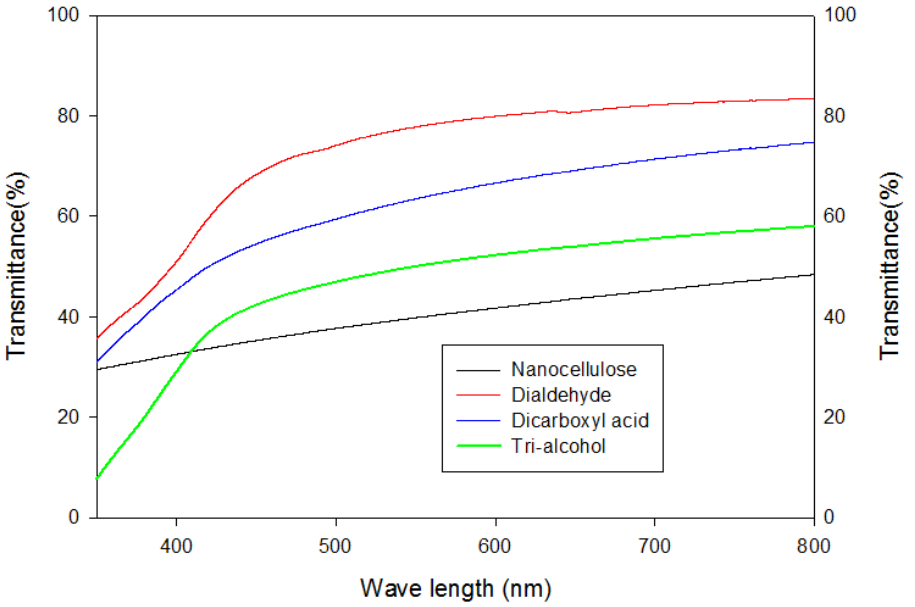

Fig. 4.26: Transparency comparison of NCC and functionalized NCC

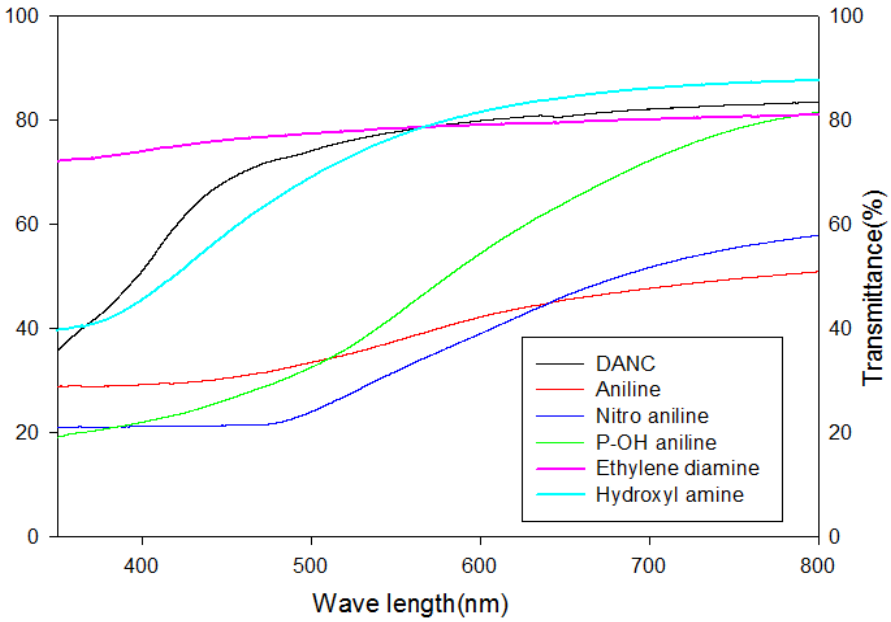

Fig. 4.27: Transparency comparison of DANC and derivatized NCC

4.12 Conclusion

Nanocrystalline cellulose was successfully prepared by sulfuric acid hydrolysis from microcrystalline cellulose. Which was also successfully functionalized into dialdehyde with selective periodate oxidizing agent. The dialdehyde nanocellulose was further converted to dicarboxylated and tri-hydroxyl nanocellulose with sodium chlorite, and sodium borohydride respectively. The dialdehyde nanocellulose was grafted with some model aliphatic and aromatic primary amines through reductive amination reaction in aqueous media.

FESEM micrographs of NCC and all modified NCCs showed that the diameter of nanocrystals has wide range of distribution but the size of most of the 'cross-lined fiber' nanocrystals lies within the range 100-300 nm in length and 10-20 nm in diameter. The dialdehyde nanocellulose and dicarboxylated nanocellulose were found more dispersive in aqueous media than NCC and it also shown higher thermal stability and transparency than NCC.

Different chemical methods, FTIR and ^{1}HNMR spectra confirmed the conversion of NCC to different functional groups and amine derivatives. The XRD results showed that NCC and its all modified products are crystalline in nature where crystallinity index of modified NCCs was decreased compare to NCC which indicates that no rearrangement of the cellulose structure into another crystalline form occurred. These amine crosslinked fibers also showed improved thermal stability and transparency than NCC. The unique characteristics of these fibers are very promising for their potential applications in composites, packaging and other technologies.

So, preparation of nanocrystalline cellulose and its functionalization and derivatization were successfully done in this work and the results obtained is highly promising because it suggests the possibility of incorporation of wide variety of different functional groups like amine, primary alcohols, shiff base, fluorescent dyes etc. in the DANC or the acid derivatives on DANC for a wide variety of novel application of NCC. This oxidation and reduction methodology can be further utilized to synthesize cellulose nanowhisker carrier molecules for drugs and biomolecules. This methodology also provides a new supramolecular cellulose nanostructure that complements the advances in the synthesis of cellulose whiskers and will undoubtedly lead to new applications for composites, drug delivery and as a template for the

synthesis of spherical structures. In conclusion, periodate oxidation and reductive-amination could be a promising path to attach various amine containing compounds such as enzymes, antibiotics to the nanowhisker surfaces for potential biomedical applications.

4.13 References:

1. Bondeson, D., Mathew, A., Oksman, K. 2006. *Cellulose*, 13, 171.
2. Beck-Candanedo, S., Roman, M., Gray, D., & Gray, G. 2005. *Biomacromolecules*, 6, 1048.
3. Araki, J., Wada, M., Kuga, S., & Okano, T. 1999. *J Wood Sci*, 45:258.
4. Dong, X. M., Kimura, T., Revol, J., & Gray, D. G. 1996. *Langmuir*, 12, 2076.
5. Jackson, E. J., & Hudson, C.S. 1938. *J. Am. Chem. Soc.*, 60, 989.
6. Xiang, Q., Lee, Y. Y., Pettersson, P. O., & Torget, R. 2003. *Applied Biochemistry and Biotechnology*, 105–108, 505–514.
7. Potthast, A., Rosenau, T., & Kosma, P. 2006. *Advance in Polymer Science*, 205, 1–48.
8. Dong, X. M., Revol, J. F., & Gray, D. 1998. *Cellulose*, *5*, 19-32.
9. Fang, Y. P., Takahashi, R., & Nishinari, K. 2005. *Biomacromolecules*, 6, 3202–3208.
10. Hofreiter, B. T., Wolff, I. A., & Mehltretter, C. L. 1957. *J. Am. Chem. Soc.,* 79 24, 6457–6460.
11. Kim, U. J., Kuga, S., Wada, M., Okano, T., & Kondo, T. 2000. *Biomacromolecules*, 1, 488–492.
12. Yuen, S. N., Choi, S.M., Phillips, D. L., & Ma, C. Y. 2009. *Food Chem,* 114, 1091-1098.
13. Keshk, S. M. A. S. 2008. *Carbohydr Polym*, 74, 942-945.
14. Fan, Q. G., Lewis, D. M., & Tapley, K. N. 2001. *Journal of Applied Polymer Science*, 82, 1195–1202.
15. Ant-Wuorinen, O., & Visapaa, A. 1963. *Paperi ja Puu,* 45, 81.
16. Calvini, P., Gorassini, A., Luciano, G., & Franceschi, E. 2006. *Vibrational Spectroscopy*, 40, 177–183.
17. Yuan, H. H., Nishiyama, Y., Wada, M., & Kuga, S. 2006. *Biomacromolecules* 7(3), 696–700.
18. Rajalaxmi, D., Elder, T., & Ragauskas, A. J. 2012.*Cellulose*, 19, 2069-2097.

19. Nishiyama, Y., Langan, P., & Chanzy, H. 2002. J Am Chem Soc, 124, 9074–9082.
20. Chen, W. S., Yu, H. P., Liu, Y. X., Chen, P., Zhang, M. X., & Hai, Y. 2011.*Carbohydr. Polym,* 83, 1804-1811.
21. Wada, M., Heux, L., & Sugiyama, J. 2004. *Biomacromolecules,* 5, 1385-1391.
22. Maren, R., & William, T. W. 2004. *Biomacromolecules,* 5, 1671-1677.
23. Rowen, J. W., Forziati, F. H., & Reeves, R. E. 1951. *J Am Chem Soc*, 73:4484
24. Duchemin, B., Newman, R., & Staiger, M. 2007. *Cellulose*, 14, 311–320.
25. Varma A. J., & Chavan, V. B. 1995. *Polym Degrad Stab*, 49, 245–250.
26. Kim U.J. & Kusa, S. 2001. *Thermochim Acta*, 369, 79.
27. Julien, S., Chornet, E., & Overand, R. P. 1993. *J. Analytic. Appl. Pyrol.,* 27, 25-43.
28. Vicini, S., Princi, E., Luciano, G., Franceschi, E., Pedemonte, E., Oldak, D., Kaczmarek, H., & Sionkowska, A. 2004. *Thermochim Acta*, 418, 123.
29. Mandal, A., & Chakrabarty, D. 2011. *Carbohydr. Polym,* 86, 1291-1299.
30. Kumar, A., Negi, Y. S., Bhardwaj, N. K., & Choudhary, V. 2012. *Carbohydr. Polym,* 88, 1364-1372.
31. Wang N, Ding, N. Y., & Cheng, R. S. 2007. *Polymer*, 48, 3486-93.
32. Wilham, C. A., McGuire, T. A., & Mehltretter, C. L. 1971. *Starch*, 23, 201–203.